Geoderma 441 (2024) 116761

Contents lists available at ScienceDirect

Geoderma

journal homepage: www.elsevier.com/locate/geoderma

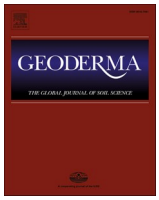

Modelling biochar long-term carbon storage in soil with harmonized analysis of decomposition data

Elias S. Azzi [a,*], Haichao Li [b], Harald Cederlund [c], Erik Karltun [b], Cecilia Sundberg [a]

[a] Department of Energy and Technology, Swedish University of Agricultural Sciences (SLU), Uppsala, Sweden
[b] Department of Soil and Environment, Swedish University of Agricultural Sciences (SLU), Uppsala, Sweden
[c] Department of Molecular Sciences, Swedish University of Agricultural Sciences (SLU), Uppsala, Sweden

ARTICLE INFO

Handling Editor: B. Minasny

Keywords:
Biochar persistence
Biochar carbon modelling
Durability
Soil carbon sequestration
Temperature sensitivity (Q_{10})

ABSTRACT

The climate change mitigation benefits of biochar systems arise largely from carbon storage in biochar. However, while biochar is increasingly recognized as a carbon dioxide removal technology, there are on-going scientific discussions on how to estimate the persistence of biochar carbon when biochar is used in soils. Estimates vary from decades to millennia, building on different modelling approaches and evidence. Here, we revisited the persistence estimates derived from extrapolation of biochar incubation experiments, with the aims of making incubation data available, modelling choices transparent, and results reproducible. An extensive dataset of biochar incubations, including 129 biochar decomposition time series, was compiled and is made available alongside code for its analysis. Biochar persistence correlations were sensitive to data selection procedures and to the curve fitting modelling step, while soil temperature adjustments methods had less impact. Biochar H/C ratio remained the main predictor of biochar persistence, in line with previous research, regardless of the extrapolation assumptions (multi-pool exponential functions or power function) used in curve fitting. The relation between H/C and percentage of biochar carbon remaining after 100 years (BC_{100}) was better explained by a power model than a linear model, with R^2 values between 0.5 and 0.9. Using multi-pool exponential functions, estimated BC_{100} varied between 90 % and 60 % for H/C from 0 to 0.7. However, using power functions, BC_{100} was constrained between 90 % and 80 % for the same H/C range. Additional information about the biochar, the pyrolysis conditions or the environmental incubation conditions did not significantly increase explained variance. Notably, the dataset lacks observations at H/C ratios below 0.2, of biochar made from manure and biosolids, biochar from processes other than slow pyrolysis, field studies, and incubation temperatures below 10 °C, which should guide future experimental work. The detailed analysis performed in this study does not cast doubts on the longevity of biochar carbon storage; rather, it confirms previous knowledge by critically examining the modelling, elucidating the assumptions and limitations, and making the analysis fully reproducible. There is a need for further interdisciplinary work on integration of various theories and approaches to biochar persistence, ultimately leading to the formulation of policy-relevant conclusions.

1. Introduction

Biochar is a charcoal-like material, obtained from biomass through pyrolysis, and used primarily as a soil amendment to improve soil properties and sequester carbon (Lehmann et al., 2015; Woolf et al., 2010). The persistence of biochar carbon in soil is a critical aspect for biochar to serve as a climate change mitigation strategy (IPCC, 2018; Tisserant and Cherubini, 2019). Over the last two decades, the persistence of biochar carbon, also referred to as biochar persistence, permanence, or stability[1] in previous research, and as biochar carbon storage durability in policy context, has been studied from multiple perspectives (Ascough et al., 2018; Bowring et al., 2022; Woolf et al., 2021). In essence, assessing the persistence of biochar carbon revolves around studying the fate of biochar once it has been placed in a soil environment, and more specifically quantifying the amount of carbon that is returned to the atmosphere over time, primarily as carbon

* Corresponding author.
E-mail address: elias.azzi@slu.se (E.S. Azzi).

[1] Note that the term "stability" is often used in combination with a qualifier, e.g. thermal stability (resistance to decomposition when exposed to high temperatures), chemical stability (exposure to chemicals), or biological stability (exposure to microbial activity).

https://doi.org/10.1016/j.geoderma.2023.116761
Received 10 October 2023; Received in revised form 19 December 2023; Accepted 20 December 2023
Available online 30 December 2023

dioxide.

1.1. Current understanding, empirical evidence, and modelling approaches

The persistence of biochar carbon varies with the properties of biochar, which result from the pyrolysis process conditions and the biomass type, but also varies with the environmental conditions to which biochar is exposed (Lehmann et al., 2021). Importantly, since biochar is a term used to describe a continuum of materials with different degrees of aromatic structure condensation, biochars do not necessarily have the same persistence. Biochars with a higher degree of fused aromatic carbon structures are less prone to microbial decomposition than fresh biomass and lightly charred materials. In soils, biochar is subject to multiple processes of degradation, protection, and transport to other compartments (e.g. nearby topsoil, subsoil, groundwater, rivers and sediments) (Lutfalla et al., 2017; Santos et al., 2022). These processes are affected by multiple factors like soil temperature, hydrological regime, texture, and management.

Biochars are estimated to be at least one to two orders of magnitude more persistent in soils than the parent biomass (Lehmann et al., 2021). However, although biochar is increasingly recognised as a carbon dioxide removal method (Canadell et al., 2021), knowledge and evidence available are not sufficient to provide a quantification of biochar carbon persistence that captures all relevant processes and variations in biochar properties and environmental conditions. A wide range of biochar carbon persistence estimates have been proposed, supported by different empirical evidence, modelling approaches and theories:

i) The biochar carbon persistence is estimated to be in the range of decades. This builds upon in-field observations (Leal et al., 2019; Ventura et al., 2019, 2014) and soil carbon modelling (Pulcher et al., 2022) for specific biochar types.
ii) A large share of carbon remains in storage for at least 100 years. Assuming that biochar remains in the topsoil where it was applied and is continuously subject to microbial decomposition, this 100-year permanence factor can be derived from the biochar's molar hydrogen to organic carbon (H/C_{org}) ratio and the soil temperature at site of use (Woolf et al., 2021). This builds upon an array of incubation studies, reviews, and models published in the field of soil science (see section 1.2).
iii) A certain share of biochar carbon is thought to remain in storage for longer than millennia. This builds upon various arguments, such as the supposed chemical and biological "inertness" of large aromatic structure in biochars characterised using various techniques (Ascough et al., 2009; Crombie et al., 2013; Harvey et al., 2012; Petersen et al., 2023), evidence of archaeological and historical remains (Ascough et al., 2020; Glaser et al., 2001), global pyrogenic carbon transport and stock models (Bird et al., 2015; Bowring et al., 2022).

The focus of this work is primarily on advancing the study of biochar carbon persistence derived from incubation experiments.

1.2. Persistence estimates derived from biochar incubation studies and research gaps

Decomposition of biochar in soils has been studied via incubation experiments (e.g. Budai et al., 2016; Zimmerman and Ouyang, 2019), has been the object of several reviews (Leng et al., 2019a,b; Spokas, 2010; Wang et al., 2016; Woolf et al., 2021), and attempts have been made to correlate permanence factors to biochar properties or pyrolysis temperature (Budai et al., 2013; IPCC, 2019; Rodrigues et al., 2023; Singh et al., 2015; Spokas, 2010; Woolf et al., 2021; Zimmerman, 2010). These assessments however, although broadly agreeing on the persistent nature of biochar, made different persistence quantifications, used partly different datasets and methodologies, and were left with high unexplained variance.

The procedure for analysing and extrapolating biochar decomposition data involves multiple steps, conceptually summarized in Fig. 1. First, data from short-term incubation experiments are compiled into a consistent dataset. Then, the decomposition data is extrapolated to longer time scales using curve fitting procedures, estimates of permanence are calculated, and various recalibrations are applied. Finally, correlations between permanence estimates and other information in the dataset are searched for. Ultimately, the resulting correlations can be adjusted for a specific policy context, e.g. project-specific carbon accounting or national inventory guidelines. Previous assessments of biochar persistence derived from incubations have used similar procedures, with several limitations and research gaps.

Data availability and reproducibility. Previous assessments of biochar incubation data did not publish their datasets of the incubation data, nor the detailed code used for performing the modelling. The data reported was usually limited to the estimated permanence and a few experimental variables. Traceability between permanence assessments and the individual observation in original publications was sometimes not possible. This hindered reproducibility and additivity of science.

Curve-fitting. Incubation studies report the amount of carbon lost at the end of the incubation period and other characteristic metrics derived from analysis of the decomposition time series, such as mean residence times[2] (MRT, i.e. time after which 63 % of initial carbon is released), half-lives[2] ($t_{1/2}$, i.e. time after which 50 % of initial carbon is released) or 100-year permanence factors (BC_{100}, i.e. fraction of carbon remaining after 100 years). These characteristic metrics are obtained via curve fitting, i.e. a process to adjust a mathematical function with a limited number of parameters to time series of decay rates or cumulative carbon losses (Weihermüller et al., 2018). Curve fitting is an optimisation problem that does not always have a unique solution, and which can be sensitive to both irregularities in experimental data and assumptions made. Hence, it is critical to disclose what algorithm, initial conditions, and fitting constraints were used and how the quality of the selected fit was assessed. This has usually been inadequately reported in biochar incubation studies, which limits reproducibility (Weihermüller et al., 2018).

In addition, the type of model used in curve fitting (e.g. single, double, triple or power exponential models) has a strong influence on persistence estimates (Bird et al., 2015; Zimmerman et al., 2011). The use of at least double pool models has been recommended for biochar (Lehmann et al., 2021), while triple pool models were considered difficult to fit due to too short incubation times (Bird et al., 2015). Other types of decay models have usually been left out from persistence modelling.

Soil temperature adjustment for biochar. Biochar incubation experiments have been performed at different soil temperatures, varying from 10 °C to 60 °C. The effect of temperature on decomposition is twofold: i) higher soil temperatures are associated with higher degradation rates, and ii) more complex molecules like biochar have a higher relative temperature sensitivity than easily degradable organic matter like sugars (Davidson and Janssens, 2006). For biochar, Lehmann et al. (2015) suggested to recalibrate the decay rates to a common soil temperature using a temperature dependent Q_{10} relationship derived from former incubation studies (Cheng et al., 2008; Nguyen et al., 2010; Zimmermann et al., 2012) and this approach was then applied in Woolf et al. (2021). However, the adjustment method is associated with high

[2] Note that half-life and mean residence time are technically referring to single first order kinetics (SFO, i.e. single exponential models) or individual pools in multi-pool models, while in the context of non-SFO kinetics (e.g. double exponentials, power model), those quantities are more accurately referred to as 50%-degradation time (DT_{50}) and 63%-degradation time (DT_{63}), respectively. For simplicity, we use the terms half-life and mean residence time.

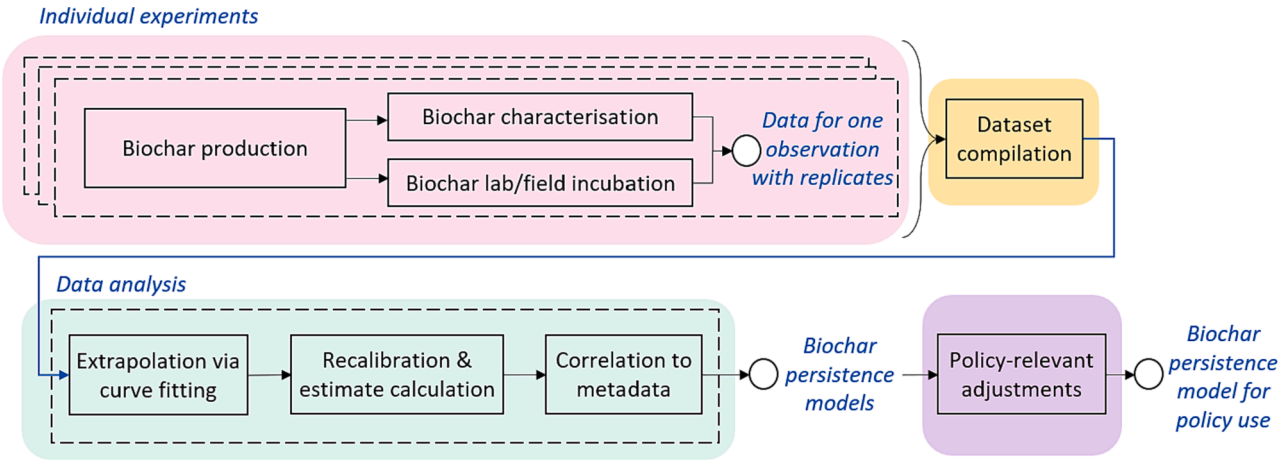

Fig. 1. From measuring a flux of carbon dioxide emission to calculating correlations between estimated persistence (or durability) and experimental variables: individual experiments, dataset compilation, data analysis, and policy-relevant adjustments.

uncertainties, limited data at low temperatures, and is thought to underestimate decay rates at low temperatures (Elsgaard and Eriksen, 2023).

Correlation search. Most previous assessments of biochar persistence focused on estimates expressed as a 100-year permanence factor, an *n*-year permanence factor, MRT, or $t_{1/2}$. Correlations with these persistence estimates were in most cases univariate (using a single parameter, e.g. H/C_{org} ratio, pyrolysis temperature) and used linear regressions; although Rodrigues et al. (2023) recently introduced a power model. No attempts at using multivariate regressions have been published, to our knowledge. Furthermore, data retained or excluded from a correlation model was not systematically justified, and extrapolation of the predictions to ranges where data points are limited were not discussed.

1.3. Aim of this work

One of the main issues in evaluation of biochar persistence through incubation studies is the lack of an open and exhaustive dataset of biochar decomposition experiments that can be updated whenever new data are collected. Published data are sometimes not transparent regarding data preparation and processing toolchain, which makes application of modelling choices and reproducibility of scientific results difficult. Thus, our first aim was to rectify this by establishing such a dataset and toolchain, thereby also enabling refined analysis and discussion on modelling choices.

The second aim was to analyse different modelling choices and attempt at refining existing biochar persistence models. More specifically, the objectives were to:

i) Analyse the effect of different curve fitting strategies and the meaning of different types of fitting functions (exponential and power functions).
ii) Analyse the effect of different temperature adjustment methods.
iii) Reproduce and critically analyse previously suggested correlations between biochar persistence and H/C_{org} ratio, at any time horizon and soil temperature.

2. Material & methods

A dataset of previously published biochar decomposition incubation data was compiled (2.1) and used for an exploratory analysis (2.2). A modelling toolchain was developed and applied to perform various analyses of the dataset (2.3).

2.1. Dataset construction

To achieve modelling transparency and reproducibility, the dataset was built following principles that are detailed in supporting information (SI, Section 1). Key aspects include: i) for an observation to be included in the database, its incubation data must be available either as time series of the decay rate or cumulative carbon loss, averaged for the experimental replicates, so that curve fitting can be performed; ii) collection of data describing the experimental conditions, here after called *metadata*, must be extensive to support result interpretation; and iii) all data in the dataset shall be associated with contextual information, to explain whenever relevant, from where data were sourced (e.g. unpublished data, obtained from authors) and if any modification or assumption were made (e.g. pyrolysis temperature not measured, but value from literature suggested by authors was reported).

The dataset was structured in four tables, each table containing multiple fields (Fig. 2). The tables were named "articles" (with 16 fields), "data" (26 fields, although only 4 were consistently populated), "metadata" (65 fields) and "validation" (109 fields). Each field is described in a database schema, which is provided in machine- and human-readable formats (json, html) (Section 2 in SI). The dataset is saved as a Microsoft Excel file but can also be exported to other formats. Additional data are also provided in separate files, e.g. data of Q_{10}-values for temperature dependence of biochar decomposition and data from previous persistence assessments (IPCC, 2019; Lehmann et al., 2021; Wang et al., 2016; Woolf et al., 2021).

For the data compilation, articles containing biochar incubation data were identified. This identification started from existing assessments (Andrade et al., 2022; Budai et al., 2013; IPCC, 2019; Spokas, 2010; Wang et al., 2016; Woolf et al., 2021) and was further extended mainly by literature searches (direct search[3], citing literature, search alerts on previous incubation studies, or direct communication with authors). Bibliographic information was saved, including e.g., open-source license information or copyright, digital object identifier, number of observations per article. Then, for each article, the individual observations were identified. For consistency and backward traceability, each observation was given a unique identifier number and a name corresponding to its given name in the original article. Whenever possible, a mapping between our data and data from former assessments (IPCC, 2019; Lehmann

[3] Scopus search string: TITLE-ABS-KEY ("biochar stability" OR "biochar decay" OR "biochar mineralisation" OR "biochar degradation" OR "biochar incubation"). Latest search done in October 2022. This search string retrieved many but not all studies included in this work. Several articles were identified from other publications or direct contact with researchers.

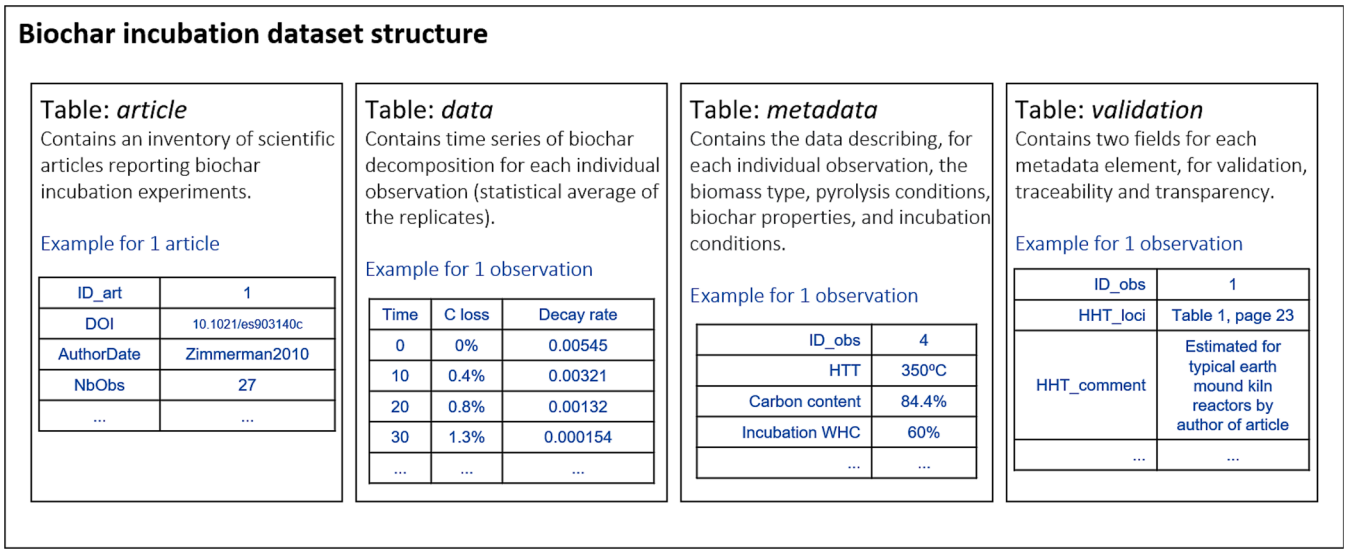

Fig. 2. Simplified structure of the biochar stability database, its four tables and example of contents for each table. DOI: Digital Object Identifier, HTT: Highest Treatment Temperature, WHC: Water Holding Capacity.

et al., 2021; Woolf et al., 2021) was also established, to enable comparisons with previous assessment at the level of individual observations. Then, for each unequivocally identified observation, the decomposition data and metadata were extracted manually. If needed, figures were digitised or contact with the authors was established to access non-published data.

As a result, the dataset contains information for 134 observations (129 observations from carbonized materials, and 5 from associated biomass controls), collected from 17 articles where biochar decomposition was measured separately from the background soil organic matter decomposition (e.g. using isotopic techniques or incubation in pure sand) (Aubertin et al., 2021; Budai et al., 2016; Fang et al., 2019, 2014; Herath et al., 2015; Kuzyakov et al., 2014; Liu et al., 2020; Major et al., 2010; Rasse et al., 2017; Santos et al., 2021; Singh et al., 2015, 2012, Ventura et al., 2019, 2014; Wu et al., 2016; Zhu et al., 2019; Zimmerman, 2010). The biochar decomposition time series (decay rates, cumulative carbon lost or remaining) have not been included in a published dataset so far; only the estimated 100-year biochar stability (IPCC, 2019; Lehmann et al., 2021) or the decay model parameters have been reported (Woolf et al., 2021). Metadata describing the experiments totalled about 8000 data elements. The most recent previous assessments had 87 observations, with much fewer metadata elements (ca 350) (Lehmann et al., 2021; Woolf et al., 2021). In addition, the dataset includes bibliographic information of 56 articles that performed biochar incubation, but those studies did not differentiate the biochar carbon losses from background soil respiration. Consequently, data were not extracted from those articles.

2.2. Exploratory data analysis

An exploratory data analysis was performed with the goal of identifying existing correlations between variables, potential data gaps or inconsistencies. A second goal was to guide future biochar incubations. Scatter plots, ternary plots, histograms, Pearson correlation matrices, distance correlation matrices, and principal component analysis (PCA) were used to analyse the metadata, the decomposition data, and other variables calculated from these data (e.g. average of decay rate over given time range, calculated dry-ash free elemental composition). The data exploration was performed in python (v3.9) using several libraries, mainly pandas (McKinney, 2010; pandas development team, 2020), numpy (Harris et al., 2020), scipy (Virtanen et al., 2020), scikit-learn (Pedregosa et al., 2011), matplotlib (Hunter, 2007), and ternary (Harper, n.d.).

2.3. Modelling toolchain development and analyses

We developed an open-source modelling toolchain in python to perform the most common data analysis steps, including data selection procedures, curve fitting, persistence estimate calculation, soil temperature adjustment, search for correlations, and various static and interactive visualisations. This modelling toolchain is released as a python library with its documentation and demonstration notebooks.[4] The sections below detail some of the key modelling steps and the analyses performed, for curve-fitting (2.3.1), soil temperature re-calibration (2.3.2), persistence estimate calculation (2.3.3), and search for correlations (2.3.4).

2.3.1. Curve fitting of incubation data

The curve-fitting procedures developed allow for specifying and disclosing modelling choices (e.g. initial conditions, algorithm and library, constraints, model function). The procedures report the fitted variables, their uncertainty and correlations, the residuals, and various goodness-of-fit metrics (e.g. sum of squared residuals, Bayesian information criteria, Durbin-Watson score). Several physical checks are also applied, which can be used to further identify realistic fits (e.g. positivity of all decay rates, positivity of pool sizes, individual pool sizes below 100 %) or rather well constrained fits (e.g. standard deviation of fitted parameter smaller than parameter value, in absolute value). All the fitting information is saved for each observation and figures can be plotted to visually inspect the quality of fitted curves. This allows all observations included in the dataset to be analysed using the same procedure, a limitation previously highlighted (Weihermüller et al., 2018).

These procedures were applied to the dataset, using multiple model functions (single, double, and triple exponential, in both constrained and unconstrained forms, and a power model (Zimmerman, 2010), see Section 3.1 in SI for parametrisation of each model function), several fitting algorithms (Levenberg-Marquardt and Trust Region Reflective algorithms, as implemented in *scipy*; and default algorithm implemented in *lmfit*), and five sets of initial conditions (different for each type of

[4] GitHub repository for biocharStability library: https://github.com/SLU-biochar/biocharStability.

exponential model function, see SI for numerical details). Best fits were then selected under different strategies (Table 1). All fits and best fits were analysed and compared to the fitted data reported in Woolf et al. (2021). Uncertainty from curve-fitting was also propagated on the fitted decomposition time series using 1st-order Taylor series expansion (Section 3.1 in SI), whenever possible.

2.3.2. Soil temperature adjustment

Three soil temperature adjustment methods were implemented and compared: a) the existing Q_{10} method (Lehmann et al., 2015; Woolf et al., 2021), b) a stepwise Q_{10} method and c) an exponential method. The two new methods, b) and c), are attempts to improve the soil temperature adjustment and overcome limitations of the existing Q_{10} approach a).

$$Q_{10}(T) = 1.1 + 12.0\ exp^{-0.19T} \tag{1}$$

$$f_{1,2} = \frac{k_2}{k_1} = (Q_{10}^{avg})^{\frac{T_2-T_1}{10}} \text{ where } Q_{10}^{avg} = \frac{1}{T_2 - T_1}\int_{T_1}^{T_2} Q_{10}(T)dT \tag{2}$$

The biochar Q_{10} method (a) relies on a temperature dependent Q_{10} factor, derived from a series of biochar incubations (Eq. (1), which is then used as shown in Eq. (2) to convert decay rates from one temperature to another. Although symmetric (i.e. $f_{1,2}{*}f_{2,1} = 1$), this relationship has an unexpected behaviour when doing multiple temperature conversions (i.e. $f_{1,2}{*}f_{2,3} \neq f_{1,3}$, see Section 4 in SI for a numerical example). In addition, attempts to reproduce the Q_{10} values that were part of the dataset used to parametrize Eq. (1) from the original Nguyen et al. (2010) study were unsuccessful.

The stepwise Q_{10} method factor is a slight modification of the method above that still uses the Q_{10} relationship in Eq. (1). However, instead of converting decay rates between two temperatures (from T_a to T_b) in one step, the conversion is done in equal steps s (Eq. (3). We noted that when s was small enough (s = 0.001 °C), the relationship converges towards a function with the expected mathematical property (i.e., $f_{1,2}^{s}{*}f_{2,3}^{s} = f_{1,3}^{s}$, see numerical example in Table S3 in SI).

$$f_{a,b}^{s} = \frac{k_b}{k_a} = \prod_{i=0}^{n-1} f_{i,i+1} = \prod_{i=0}^{n-1}\left(\frac{1}{s}{*}\int_{T_a+i{*}s}^{T_a+(i+1){*}s} Q_{10}(T)dT\right)^{\frac{s}{10}} \tag{3}$$

Lastly, the exponential method builds upon a simple relationship between biochar decay rates and incubation temperature, directly derived from the dataset compiled in this study, and similar to the approach originally suggested in Cheng et al. (2008). For all observations with a H/C ratio below 0.7 and pyrolysis temperature above 400 °C (to exclude non biochar observations), the average decay rate over the 2nd year of incubation was calculated. This average decay rate was then plotted against incubation temperatures, and an exponential relationship derived, resulting in the parametrization in Eq. (4) and the conversion factor in Eq. (5), where temperature T is expressed in degree Celsius. This parametrisation corresponds to Q_{10} values of 2.0, 1.6, and 1.5 for temperatures of 0, 10, and 20 °C, respectively.

$$k(T) = 0.9\ exp^{0.02T} - 0.7 \tag{4}$$

$$f_{a,b}^{e} = \frac{k_b}{k_a} = \frac{0.9\ exp^{0.02T_b} - 0.7}{0.9\ exp^{0.02T_a} - 0.7} \tag{5}$$

The three approaches were compared numerically for a range of initial and target temperatures, by comparing the conversion factors $f_{a,b}$ obtained for the incubation temperatures present in the dataset and by comparing the effect on the 100-year permanence of multi-pool exponential fits from the dataset (section 3.3 below and section 8 in SI).

2.3.3. Calculation of persistence estimates

To identify potentially relevant correlations with the metadata available, we expanded the persistence estimates (i.e. indicator derived from curve fitting) from commonly used MRT, $t_{1/2}$ and BC_{100} to also include: i) amounts of carbon remaining at 1, 2, 5, 10, 20, 30, 40, 50, 75, 100, 200, 500 years, and ii) annual average decay rates in the n-th year (where n also varies from 1 to 500 years). These persistence estimates can be calculated from the fitted data, for any observation, at any time horizon, soil temperature, and temperature adjustment method.

2.3.4. Search for persistence correlations

Finally, functions were developed to correlate the available metadata to persistence estimates. This includes calculation of distance correlation matrices, but also functions to perform linear correlations, as well as non-linear, multi-variate, and multi-target correlations. The main non-linear models implemented were power functions, sigmoid functions, piece-wise linear functions, and tree-based methods like random forest regressors (Breiman, 2001).

Data selection. Persistence correlation analyses were performed on different subsets of observations: i) all observations, ii) excluding singular observations, and iii) excluding singular observations and outliers. Singular observations refer to observations where modelling issues arose (e.g. unreliable fits) or which did not meet certain criteria (Table 2). For each singular observation, reasons for classification as singular are reported in Table S4 (Section 9 in SI) and are explained in results (sections 3.2 and 3.3). The few remaining outliers are observations that met all selection criteria, but still resulted in unexplainable low persistence estimates (i.e. 0 % remaining after 100 years for H/C values where the majority of observations had much higher remaining fractions). Singular observations and outliers are shown separately on graphs.

BC_{100} and H/C correlation. Linear regressions were computed on the different subsets of data, to re-produce the same type of relationship as previously published. A clipped power model was also introduced (Eq. (6)), with four parameters: M, a, b, α), to describe expected non-linearity in persistence and absence of persistence for very high H/C values (raw biomass). The 95 % confidence intervals were calculated by propagation of fitting uncertainty by 1st-order Taylor series expansion.

$$\begin{cases} BC_{100} = M - a(H/C)^b, \ if\ H/C < \alpha \\ BC_{100} = 0, \ if\ H/C \geq \alpha \end{cases} \tag{6}$$

Random forests. Random forests regressors were used to illustrate multi-target and multi-variate regressions. The random forests were fitted on the dataset excluding singular observations and outliers, in a descriptive way rather than in a predictive way (i.e. not using separate train/test/validation sets neither using out-of-bag methods). To limit over-fitting, the maximum depth of the decision trees was set to 5. The regressions were multi-target, meaning that the regressions would calculate simultaneously multiple persistence factors (biochar carbon remaining at any time horizon and soil temperature). The regressions were set up to use one or several variables as input data, and 39 combinations were tested in total. One regression included 24 possible metadata variables; other regressions included 1 to 3 variables (see variable combinations in Table S5, Section 10 in SI).

3. Results and discussion

3.1. Dataset exploratory analysis

The compiled dataset was explored with a focus on measured timeseries of decay rates, gaps in the dataset, and internal correlations.

Decay rate timeseries. Across all observations, measured biochar decay rates decrease with incubation time and are in the range of 10^{-4} to 1 gC yr^{-1} gC_0^{-1} (Fig. 3; Figs. S5–S6 in SI). After a few months of incubation, decay rates are from one to several orders of magnitude lower than decay rates of fresh biomass (Ntonta et al., 2022), in line with previous reports (Woolf et al., 2021) (Fig. 3). At longer incubation times (>730 days), measured decay rates for some biochars were in the range of decay rates measured for lignite (Chabbi et al., 2006) (Fig. 3).

Table 1
Strategies S1–S4 applied for selection of best-fit in curve-fitting of decomposition data. S: single, D: double, T: triple, R^2: coefficient of determination, BIC: Bayesian Information Criteria.

	S1 (constrained double exponential)	S2 (any exponential)	S3 (power)	S4 (any model)
Rationale	Reproduce results from previous studies, with mainly constrained double exponential models	Neither force double exponential, nor force sum of pools to add up to 100 %; perform additional consistency checks	Test behaviour of power model	Let best fit selector and consistency checks select best model type for each observation
Model functions	D exponentials, constrained only	S, D, T exponentials, constrained and unconstrained	Power model only	All model functions
Checks applied	- Positive decay rates - Positive pool sizes	- Positive decay rates (not applicable to power model) - Positive pool sizes (not applicable to power model) - Decay rates significantly different (not applicable to power model) - Parameters constrained		
Initial conditions	None (default)	Five sets of initial conditions per exponential model	None (default)	Five sets of initial conditions per exponential model
Best fit selector	R^2	BIC		
Algorithm/library	Levenberg-Marquardt and Trust Region Reflective algorithms, from *scipy*; and default algorithm implemented in *lmfit*			

Cumulative carbon lost at the end of the incubations ranged from 0.02 % to 22.6 %, with a median of 1.4 %, across all studies and biochar types (Table 3). Notably, the few timeseries from field decomposition studies did not have smooth exponential decay curves as laboratory incubation, but exhibited oscillations linked primarily to seasonal temperature variations (Ventura et al., 2019).

Feedstock type. Most observations were from wood-derived biochars (53 %). Other biomass types used were crop residues (25 %, mainly corncob, rice straw or wheat straw), grass (16 %, mainly miscanthus), manure, leaf and biosolids (<5% each) (Table 3). Biomass with a C_4 carbon fixation pathway e.g., maize, miscanthus or sugarcane have been commonly used as feedstock as it is an easier way to obtain an isotopically traceable biochar compared to using an actively labelled biomass.

Conversion process conditions. The vast majority of observations used biochar produced via slow pyrolysis (95 %), while only a handful of observations are available for gasification (Ventura et al., 2019, 2014), hydrothermal carbonisation or flash carbonisation (Budai et al., 2016) (Table 3). In most cases, the pyrolysis was performed in laboratory bench scale reactors, although some commercial pyrolysis reactors have also been used.

Recorded pyrolysis conditions included the highest treatment temperature (HTT, °C), the heating rate (HR, °C/min) and the residence time (RT, min) at the HTT. The HTT is nearly always reported in incubation studies, although it is recognised that HTT is difficult to determine in large scale (commercial) reactors due to non-homogenous heat distribution (Budai et al., 2016). Likewise, HR and RT are mainly reported for laboratory produced biochar where these parameters are well controlled. A common possible source of misinterpretation, for the RT, is that some studies report an overall RT inside the reactor (from start to end of pyrolysis process, possibly including drying time) while others report the RT at HTT. Here, only RT at HTT was included in the database leading to some missing data.

The reported HTT ranged from 105 °C (drying, fresh biomass incubations) to 1200 °C (gasification), with most values in the range of 400–600 °C (Fig. 4a). HR spanned between 0.1 °C/min and 51 °C/min, with a median of 7.5 °C/min. Finally, RT was mostly between 40 min and 3 h, although the effect of longer residence time was tested in some cases, with RT up to 72 h (Zimmerman, 2010). In terms of pyrolysis conditions, there is a data gap for biochars produced at higher temperatures (>600 °C). Furthermore, chars from hydro-thermal carbonisation, flash carbonisation, gasification and fast pyrolysis have mainly been incubated without isotopic techniques (Andrade et al., 2022), and are therefore underrepresented in this dataset.

Biochar elemental composition and ratios. Basic elemental composition (C, H, O, N) is reported in most incubation studies, as well as molar elemental ratios (H/C, O/C) (Fig. S7 in SI). However, it is worth noting that only 8 observations, corresponding to only 2 different biochars, have measured both the total carbon (C_{tot}) and the organic carbon (C_{org}) contents. Previous assessments most often assumed that C_{tot} and C_{org} contents were equal. This assumption was reproduced in the current dataset and explicitly reported. The difference between C_{tot} and C_{org} is likely to be negligible (<1%) for most biochars made from woody feedstocks and with a low ash content. In the present study, whenever carbon content is used in calculation, C_{org} was used unless missing, in which case C_{tot} is used to bridge the data gap. This bridged carbon content is simply noted C (e.g. H/C ratio, O/C ratio in Fig. 4b-c).

The molar H/C ratio, which indicates the average (bulk) degree of carbonisation of a biochar sample, ranged from 0.13 to 1.4, with a median of 0.54. Lower values of H/C ratio are thought to be associated with higher pyrolysis temperatures and longer residence times, but also higher persistence. We note that only 4 biochars with an H/C ratio below 0.2 (Aubertin et al., 2021; Budai et al., 2016; Rasse et al., 2017)[5] have been incubated so far, and no biochars with H/C ratios below 0.1 (Fig. 4b). This is an important data gap for the validity of biochar persistence models, as it has been reported that biochars formed at higher temperatures, resulting in H/C ratios well below 0.1, show higher degree of aromatic condensation and specific morphotypes (Petersen et al., 2023). It must also be noted that there is trade-off between production of biochars with lower H/C and maximising the biomass-to-biochar carbon yield and subsequent carbon storage potential (Rodrigues et al., 2023; Weber and Quicker, 2018).

Biochar ash and pH. Ash content was determined either at 550 °C or at 700 °C, and seldomly using both methods. Regardless of the method, the ash content varied between 0.3 % (wood) and 76 % (cow manure), with a median around 7 %. Biochar pH was mostly determined in water (a handful of observations also determined pH in a $CaCl_2$ solution), but at different char-to-water mass ratios (1:1, 1:5, 1:10, 1:20). Regardless of the ratios used, the pH of biochar varied between 6.3 and 10.8, with a median at 9.5 (excluding two hydrothermal carbonization (HTC) samples, which had lower pH values around 4.0).

Biochar chemical oxidation and other indicators. Although proposed as a persistence indicator a decade ago (Cross and Sohi, 2013) and more recently re-analysed (Liu et al., 2020), chemical oxidation of biochar has only been reported for 11 observations. Besides, the few studies reporting chemical oxidations have used different concentrations of reagents and reaction times. Likewise, emerging characterisation methods such as hydrogen pyrolysis (Ascough et al., 2009; Howell et al., 2022) or random reflectance measurements (Mastalerz et al., 2023; Petersen et al., 2023) have so far not been used to characterise biochars from incubations with separate measurement of biochar C fluxes.

[5] The biochars with H/C < 0.2 from Budai et al. (2016) and Rasse et al. (2017) are the same.

Table 2
Criteria used for classification as singular observations. For each criteria, the number of observations (n) that meet the criteria is indicated. Note that in practice, most observations met multiple criteria simultaneously.

Criteria	*n*	Remarks
Incubation duration shorter than 349 days[a]	7	Similar to previous persistence assessment (Woolf et al., 2021), it is assumed that incubations shorter than a year are not suited for long-term extrapolation. The observations include: 2 observations with 90 days (Rasse et al., 2017), the same biochars are incubated for 365 days (Budai et al., 2016) 2 observations with 164 days (Ventura et al., 2014), the same biochars are incubated for 959 days (Ventura et al., 2019) 3 observations with 200 days (Zhu et al., 2019)
Incubation temperature higher than 40 °C	20	In Fang et al. (2014), biochar was incubated at 20 °C, 40° and 60 °C. The observations at 20 °C are kept in regression analyses. See section 3.3.
Soil-less or weathered materials	4	In Aubertin et al. (2021), out of 6 observations, 2 were performed with pure biochar (soil-less) and 2 were performed with weathered biochars. These experimental setups are not directly comparable with the other experimental setups in the dataset. The 2 remaining observations are kept (incubation of non-weathered biochar-compost blends).
Accelerating decay in power model	12	Related to curve fitting issues[b]. This indicates that the fitted power model predicts an acceleration of the biochar decay rates. This usually arose when experimental data showed temporary increases in decay rates.
Single exponential as only best fit	13	Related to curve fitting issues[b]. This indicates that double and triple exponential models had too large uncertainties to be selected as best fit, and usually arose when experimental data showed temporary increases in decay rates.
Difference in BC_{100} between power and exponential model larger than 20 %	15	Related to curve fitting issues[b].

[a] The cutoff time is set to 349 days (instead of 1 year) to avoid excluding observations that have exactly a 1 year duration (n = 57), 360 days (n = 2), and 1 field observation where the last measurement is missing resulting in 349 days of incubation (Singh et al., 2015).
[b] The three criteria related to curve fitting issues overlap to a large extent, i.e. issues with power model are linked to identification of single exponential as best fit, and to large differences in BC_{100} between the two extrapolation models. They also overlap partly with high incubation temperatures.

Incubation conditions. Among the 129 biochar observations included at this stage, only 8 corresponded to biochar incubation under field conditions (Major et al., 2010; Singh et al., 2015; Ventura et al., 2014, 2019) (Fig. 4f). Most incubations were performed at a temperature between 20 and 35 °C, and a handful at other temperatures (Fig. 4d). Temperatures lower than 20 °C usually correspond to field studies, where only the annual average temperature is reported. Temperatures of 40 °C and 60 °C were used in one article to determine temperature sensitivity of biochar decomposition (Fang et al., 2014). No incubation was yet performed at temperatures below 10 °C, which is of relevance in cold climates. Incubation duration has been argued to be an important factor in the determination of biochar persistence estimates, and longer experiments usually lead to higher persistence estimates than shorter ones (Zimmerman et al., 2011). Incubation duration varied between 90 days and 3102 days (8.5 years), with a mode of 365 days and a median of 390 days (Fig. 4e). Finally, in laboratory incubations, soil moisture was set to 60–70 % of WHC in all except 5 observations where it was set to 100 % representing flooded paddy conditions (Wu et al., 2016). Effects of freeze–thaw cycles were not studied in the experiments from which the dataset was compiled.

Soil properties. Soil properties are shown in the SI (Figure S8-10, Section 6). Most soils had a sandy texture, with few clay-rich soils. Soil pH before biochar application ranged from 4.6 to 8.8 with a median of 6.8. Soil organic carbon content is also available in the database and ranged from 0 % (pure sand incubations with microbial inoculate, Zimmerman et al. (2011)) to 10 % (Andisol under permanent pasture, used in Herath et al. (2015)), with a median of 1.2 %.

Identified data gaps. Overall, the main gaps in the incubation dataset concern: i) biochars produced at temperatures above 600 °C, ii) biochars with high degree of carbonisation i.e. H/C ratios below 0.1, which is directly related to the temperature gap, iii) studies under field conditions, iv) incubations at soil temperatures below 10 °C, and v) characterisation of biochar samples using chemical and optical indicators of stability. The latter gap could partly be bridged by re-characterisation of previously incubated samples whenever these are still available.

Correlations within the dataset. Linear Pearson correlation and non-linear distance correlation were calculated for all numeric metadata in the dataset (Figure S11-S12, Section 6 in SI). These revealed expected and known correlations between biochar properties and production conditions, e.g. higher pyrolysis temperature and higher carbon content (Ippolito et al., 2020; Weber and Quicker, 2018). Further, linear Pearson and distance correlations were calculated between the cumulative carbon lost, the last measured decay rate, and all numeric metadata (Figure S13). Cumulative carbon lost and last measured decay rates, used here as simple indicator of biochar decomposition directly derived from the dataset, showed a medium level of correlation (i.e. r = 0.3 to 0.6, in absolute values) with biochar elemental composition and ratios (C, H, and O on dry as free basis, H/C, O/C), Volatile Matter, Fixed Carbon (as determined by proximate analysis), biochar pH, and soil organic matter. Notably, while linear correlation was low with pyrolysis temperature (r = 0.08 with cumulative carbon lost, r = 0.01 with last measured decay rate), non-linear correlation was higher (r = 0.38, r = 0.34).

Finally, a PCA was performed on all numerical variables, using the last measured decay rate as simple indicator of persistence (Fig. 5). The total explained variance was 53 %, indicating that the variation within the dataset is difficult to explain. The PCA only considered the numerical variables, thereby excluding information like biomass class, pyrolysis class, or incubation type. The 1st and 2nd components indicate that higher values of last measured decay rate are related to higher oxygen, hydrogen, H/C and O/C ratios, but also partly linked to higher soil organic matter and silt contents. Lower decay rates are here related to higher biochar C content, pyrolysis temperature, C/N ratio and sand content.

3.2. *Curve-fitting of incubation data*

Biochar carbon remaining as a function of time was fitted for all observations using a set of model functions, initial conditions, algorithms, and libraries, totalling 53 fits per observation. Then, four best-fit selection strategies (Table 1) were applied and compared. The analysis includes in SI a comparison with fits previously reported in Woolf et al. (2021) for a common sub-set of 66 observations (Section 7.5 and Figure S16 in SI).

Curve fitting procedure. Learnings from the curve fitting procedure are explained in Section 7 in SI and briefly summarized here. For this dataset of biochar incubations, using multiple sets of initial conditions (Table S1, Section 3.4 in SI) was useful to identify good fits. Applying physical consistency checks helped eliminating unrealistic fits and some degree of overfitting. Residuals were mostly not randomly distributed and sometimes reflected systematic patterns, indicating changes in environmental conditions (temperature) during the incubation time.

In previous work, the coefficient of determination (R^2) has commonly been used for selecting a best fit; however, this is not recommended for curve-fitting of non-linear functions and does not allow

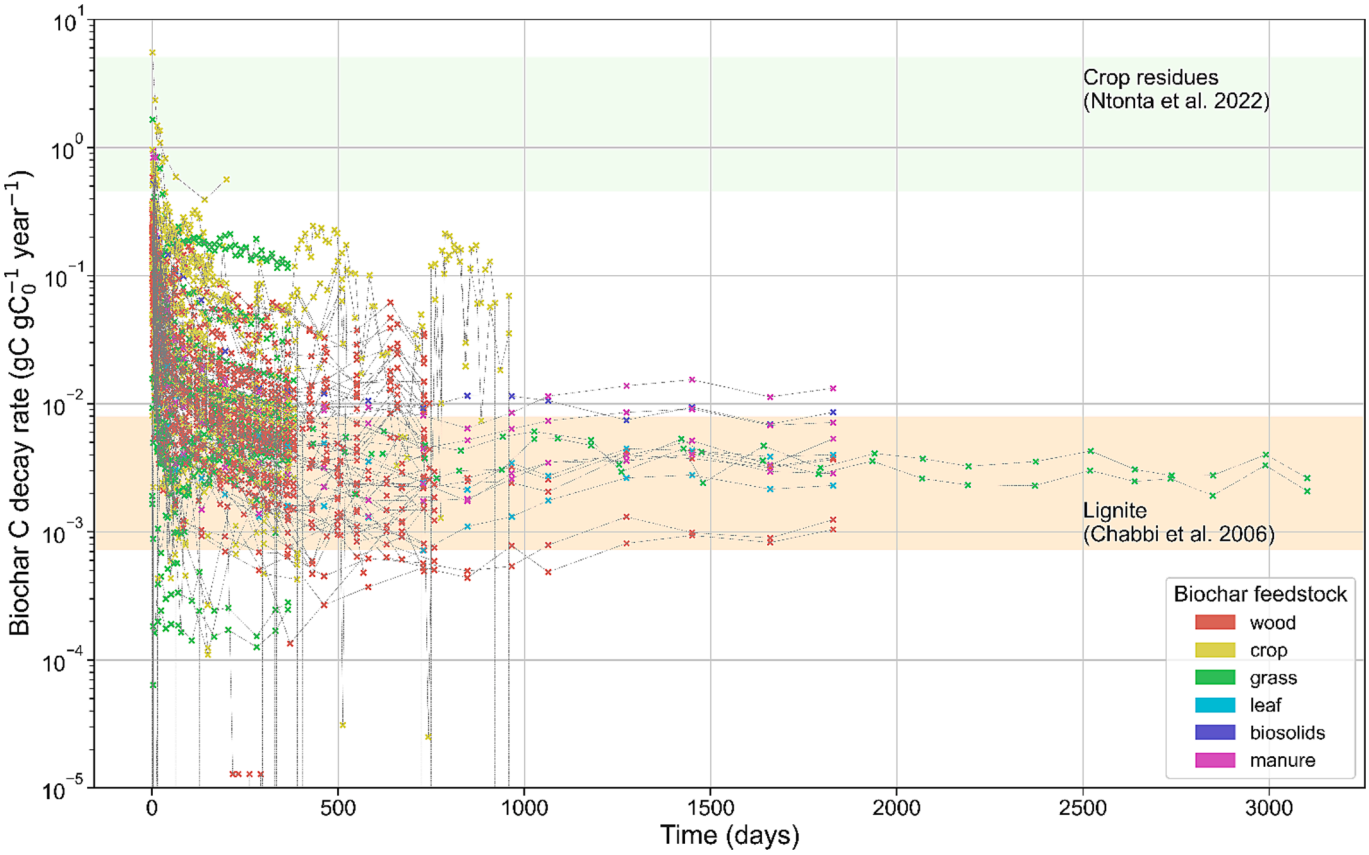

Fig. 3. Measured biochar carbon decay rates (in gC gC_0^{-1} yr^{-1}, C_0 is the amount of biochar C initially applied, logarithmic scale) for all observations included in the dataset, as average of experimental replicates. The color indicates the biomass feedstock. The upper and lower shaded areas indicate decay rates for fresh biomass residues (Ntonta et al., 2022) and for lignite (Chabbi et al., 2006), respectively. Decay rates can be converted to mgC gC_0 day^{-1} by dividing by 2.74.

Table 3
Cumulative biochar carbon lost, expressed as % of initially applied carbon, for incubations shorter than 2 years and incubations equal or longer than 2 years. Minimum, median and maximum values, calculated for different groupings of the data (all data, by feedstock classes, by pyrolysis classes, by H/C ratio). Numbers in brackets indicate the number of observations in each group (n). Cumulative carbon lost at end-of-incubation of fresh biomass is also reported from studies that incubated fresh biomass. HTC: Hydrothermal carbonization.

Grouping	Cumulative carbon lost at end of incubation (% of initially applied carbon)							
	Incubations shorter than 2 years				*Incubations longer than 2 years*			
	Min	Median	Max	*n*	Min	Median	Max	*n*
All biochar observations (129)	0.02	1.1	15.3	(72)	0.4	1.9	22.6	(57)
Feedstock classes (129)								
- Wood (69)	0.5	1.2	7	(23)	0.4	1.5	10.9	(46)
- Crop (32)	0.2	1.2	15.3	(30)	14.9	18.7	22.6	(2)
- Grass (21)	0.02	0.6	15.2	(19)	5.5	5.6	5.8	(2)
- Leaf (2)	NA	NA	NA	NA	1.2	1.9	2.5	(2)
- Biosolids (1)	NA	NA	NA	NA	8.9	8.9	8.9	(1)
- Manure (4)	NA	NA	NA	NA	2.1	4.6	7.3	(4)
Conversion process classes (129)								
- Slow pyrolysis (122)	0	1.1	15.2	(67)	0.4	1.8	10.9	(55)
- Gasification (4)	2.8	5.3	5.3	(2)	14.9	18.7	22.6	(2)
- Flash carbonisation (1)	0.5	0.5	0.5	(1)	NA	NA	NA	NA
- HTC (2)	10	12.7	15.3	(2)	NA	NA	NA	NA
Molar H/C ratio (129)								
- H/C < 0.3 (9)	0.02	0.4	2.2	(9)	NA	NA	NA	NA
- 0.3 ≤ H/C < 0.7 (93)	0.2	1	10.1	(43)	0.4	1.6	22.6	(50)
- 0.7 ≤ H/C < 1.0 (19)	0.3	1.3	4	(15)	2.2	3.1	6.9	(4)
- H/C ≥ 1.0 (6)	6.6	14.5	15.3	(5)	7.3	7.3	7.3	(1)
Fresh biomass (5)	29.4	38.7	57.3	(5)	NA	NA	NA	NA

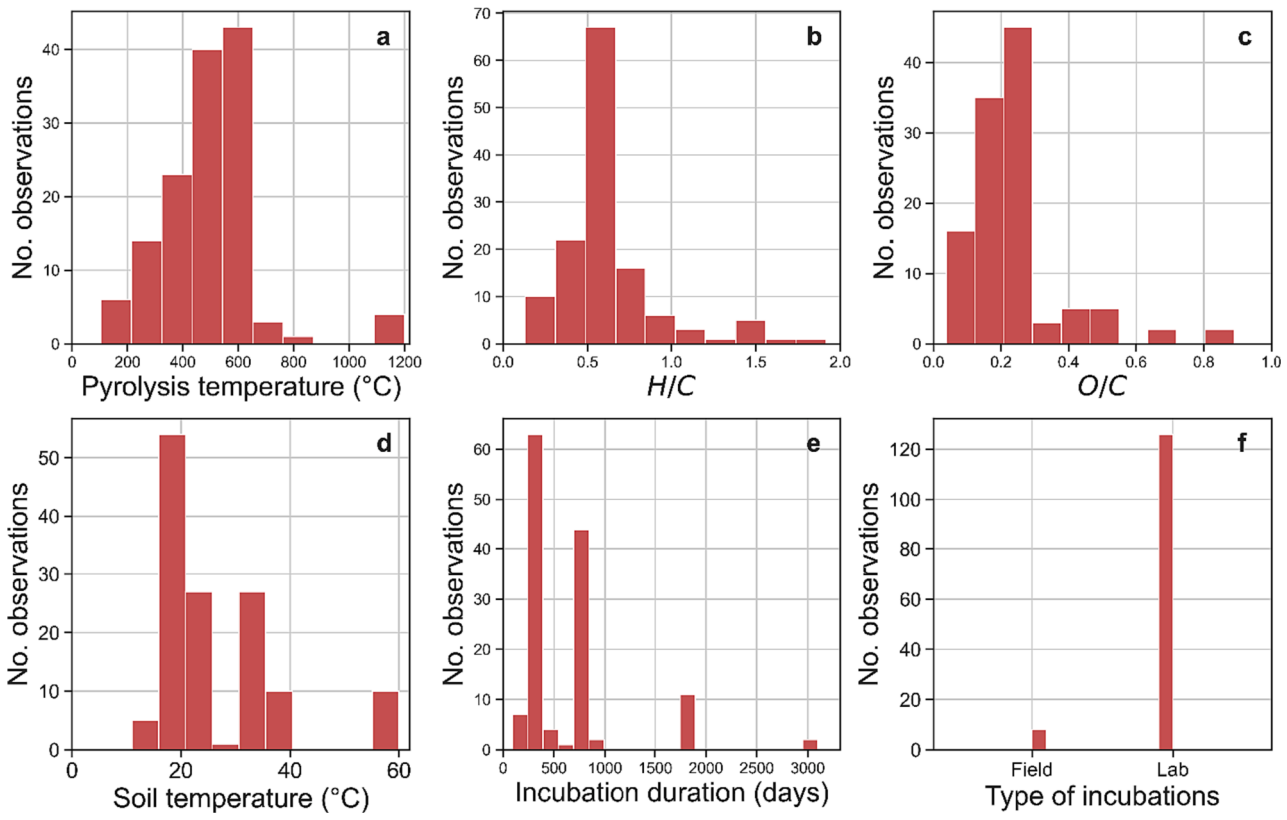

Fig. 4. Histogram of pyrolysis temperature (a), molar H/C ratio (b), molar O/C ratio (c), incubation soil temperature (d), incubation duration (e) and incubation type (f), for all biochar and fresh biomass observations included in the dataset.

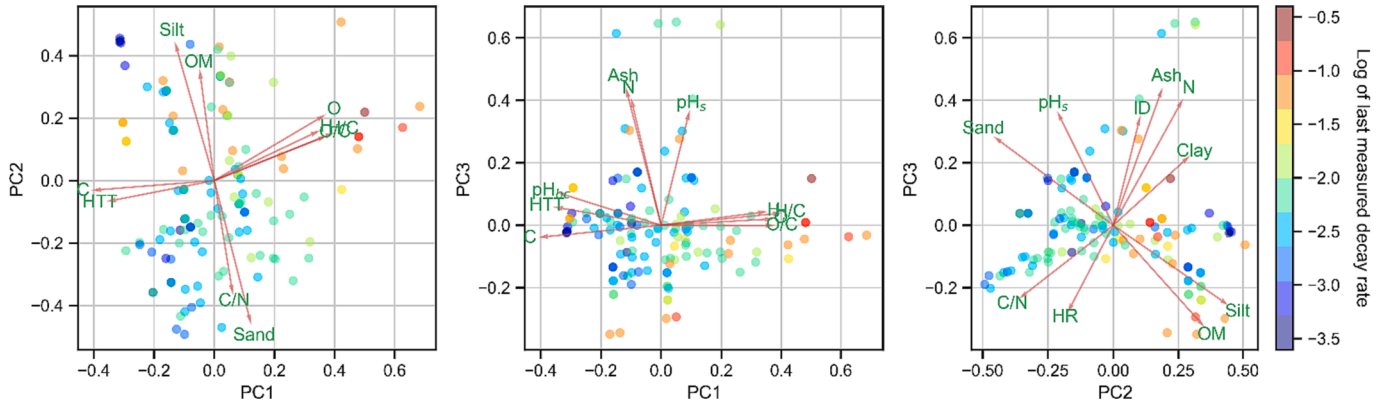

Fig. 5. Principal component analysis performed on all numeric variables in the dataset (excluding last measured decay rate and total C lost at end of incubation), with 3 components. Explained variance per component was 25%, 16%, and 12% (53% in total). The 10 most important variables are shown as arrows (HTT: highest treatment temperature; HR: heating rates; biochar elemental composition ratios: C, N, H/C, O/C, C/N; pH_{bc}: biochar pH; Ash: biochar ash content; OM: soil organic matter content; pH_s: soil pH; Sand, silt: sand and silt soil contents; ID: incubation duration). The colors indicate the last measured decay rate in logarithmic scale, for each observation (hence with variable incubation durations).

model ranking and selection (Weihermüller et al., 2018). Here, the Bayesian information criteria (BIC) was used instead: it was observed that BIC and R^2 did not yield the same rankings of fits for this dataset; but that all fits selected by BIC also had a high R^2 (>0.9).

However, even if the fitting strategies and procedures above allow the identification of best fits, those fits may still lead to results that conflict with current theories and understanding mainly because of irregularities in the incubation data, such as increasing decay rates during some parts of the incubation. This was for instance the case of some biochars incubated at 40 °C and 60 °C (Fang et al., 2014), several biochars in Budai et al. (2016), and some field studies (Figure S15, Table S4, Section 7 in SI). Therefore, it is important to visually inspect the incubation data and the fitted models. In this study, all available incubation data were included in the dataset for transparency; however, irregularities in the incubation data may be a criterium for exclusion when developing persistence correlations.

Exponential models. Previous work recommended the use of double exponential functions over single exponential functions (Woolf et al., 2021). Triple exponential functions were only rarely used. Here, strategy S2 shows that triple exponential functions (63 best fits) can be as relevant as double exponential functions (58 best fits) (Table 4). It also indicated that even single exponentials cannot be excluded in some cases

(13 best fits). However, further visual inspection revealed that single exponential best fits were mostly related to experimental time series with irregularities, and therefore high fitting uncertainties which led to exclusion of higher pool models by the checks applied. In such cases, even if the R^2 was high, the validity of the best fits may still be questioned. Last, in most cases, the constrained models were selected as best fit in S2; but in some cases, unconstrained models were selected (Table 4). This was also linked to irregularities in the experimental data.

Power models. It was possible to fit power models to all 134 observations, but five observations did not pass the constraint on parameter uncertainty (Strategy S3, Table 4). Previously, power models have been shown to yield much longer residence times than exponential models (Zimmerman et al., 2011) but have not been applied to all available biochar and biomass incubation time series.

Fig. 6a compares BC_{100} obtained with power model and exponential models, for all observations. It shows that power models can describe situations where biochar/biomass decays rapidly and yield similarly low 100-year permanence fractions as exponential models, with only a handful of exceptions (see bottom left corner in Fig. 6a). When exponential models predict high BC_{100} (>80 %), power models also predicted high (higher) BC_{100}, with few exceptions. Between those extremes, when BC_{100} from exponential models was in the range 20 %-80 %, power models tended to yield higher BC_{100} values in most cases.

Power models yield similar or slightly lower MRTs whenever exponential models yield MRTs below 500 years, but beyond this point, power models generally yield MRTs that are several orders of magnitude higher (Fig. 6b). Hence, it may be argued that for the timescales relevant in climate policy (from century to millennia), both model types seem to provide comparable results, with some notable exceptions related to irregularities in the measured decay rates (see details in section 7.4 in SI).

Overall, power models extrapolate biochar decomposition by extrapolating the observed change in decay rate during the incubation time. Under the theory that biochar is an arrangement of aromatic carbon structures where remaining biochar has an increasing chemical stability and thereby decreasing susceptibility to microbial oxidation, the power model may make more sense than a finite number of exponentials (Zimmerman et al., 2011). However, whether observed decline in decay rate reflects future decline is not obvious and constitutes an inherent assumption of power models. As for exponential models, curve fitting extrapolation highlights the need for long-enough experiments (typically > 1–2 years).

Best fits & singular observations. Overall, even if best fits were identified by the strategies applied; these may still result in unexpected or too uncertain extrapolations results. At this stage of the modelling, 32 observations from 8 articles were classified as singular observations, of which 23 were based on irregularities in the curve fitting step, 5 due only to incubation time shorter than 349 days, and 4 due only to soil-less experimental conditions (Table 2, Table S4 in SI). For the rest of this article, best fits from strategies S2 (all exponentials, with constraints) and S3 (power model, with constraints) were used.

Table 4
Statistics from best-fit selection strategies: number of model functions selected as best fit, best fits with or without initial conditions set, and library/algorithm used. NA indicates not applicable for the given fitting strategy; while a 0 indicates no results obtained for that criteria. S_c/S_u: single exponential constrained/unconstrained, D_c/D_u: double exponential constrained/unconstrained, T_c/T_u: triple exponential constrained/unconstrained, P: power model, TRF: Trust Region Reflective algorithm, LM: Levenberg-Marquardt algorithm, R^2: coefficient of determination.

	S1 (constrained double exponential)	S2 (any exponential)	S3 (power)	S4 (any model)
Functions				
- S_c / S_u	NA / NA	08-May	NA / NA	0 / 2
- D_c / D_u	134 / NA	46 / 12	NA / NA	38 / 7
- T_c / T_u	NA / NA	61 / 2	NA / NA	39 / 1
- P	NA	NA	129*	41
Initial conditions				
- Not specified	134	54	129*	83
- Specified	NA	80	NA	51
***Library*, algorithm**				
- *Scipy*, TRF	79	61	129*	94
- *Scipy*, LM	28	56	0	26
- *lmfit*, default	27	17	0	14
R²*, *min*, *max	0.94, 1.0	0.92, 1.0	0.91, 1.0	0.94, 1.0

* No best fit was found for 5 observations, due to the check on parameter standard deviation

3.3. Soil temperature adjustment

Overall, the three soil temperature adjustment methods had a similar behaviour i.e. increasing with temperature although differently, and resulted in minor differences on average (Figure S17 and section 8 in SI). The new methods both provided slight improvements of decay rate corrections at lower target temperatures, in line with unpublished results that concluded that the Q_{10} method overestimates long-term stability in soils at 0–10 °C (Elsgaard and Eriksen, 2023).

Temperature adjustment methods remain associated with large uncertainties and unknowns (Davidson and Janssens, 2006). For instance, all methods assume that biochar temperature sensitivity observed over 0–2 year of incubation informs on the temperature sensitivity of the whole extrapolated period (0 to 100 years), and that all biochars respond in a similar way. Data at lower incubation temperatures is also scarce, and temperature adjustment from high temperatures (40°, 60 °C) down to 20 °C is not well calibrated (section 8 in SI). Thus, to minimize uncertainty related to temperature adjustment, the rest of the article presents calculations at the most common incubation temperature (20 °C), and the incubations not performed at 20 °C were adjusted using the exponential method. In addition, at this stage of the modelling, 17 observations from Fang et al. (2014) with incubation temperature of either 40 °C or 60 °C were classified as singular observations (Table 2, Table S4 in SI).

3.4. Persistence correlations

3.4.1. Distance correlation matrices

Following curve fitting and temperature adjustment, persistence estimates were calculated for each observation. Correlation of persistence estimates with metadata was investigated using distance correlation matrices (Figure S18 and S19, Section 10 in SI). For exponential models (strategy S2), carbon remaining at any time correlated strongly with biochar elemental composition and molar ratios (C, H, O, H/C, (H + O) / C), biochar pH, fixed carbon, volatile matter, pyrolysis char yield, and pyrolysis temperature (r > 0.5 to 0.9). There were stronger correlations (by 0.1 to 0.3 units) between estimates of carbon remaining after short time frames (0 to 100 years) than longer ones (100 to 500 years). Both carbon remaining and annual average decay rates showed the highest correlation with total C lost during incubation time and last measured decay rate, the variable that was used as a preliminary persistence indicator in the PCA (Fig. 5). For power models (strategy S3), similar patterns were obtained but correlations were weaker at longer time horizons (by 0.1 unit). MRT and $t_{1/2}$ exhibited weaker correlations with the variables mentioned above (r < 0.4).

Overall, these correlation matrices seem to indicate that among all numerical variables, biochar elemental composition (C, H, O), molar ratios, fixed carbon, volatile matter, biochar pH, and the pyrolysis temperature are most relevant to consider for persistence estimates.

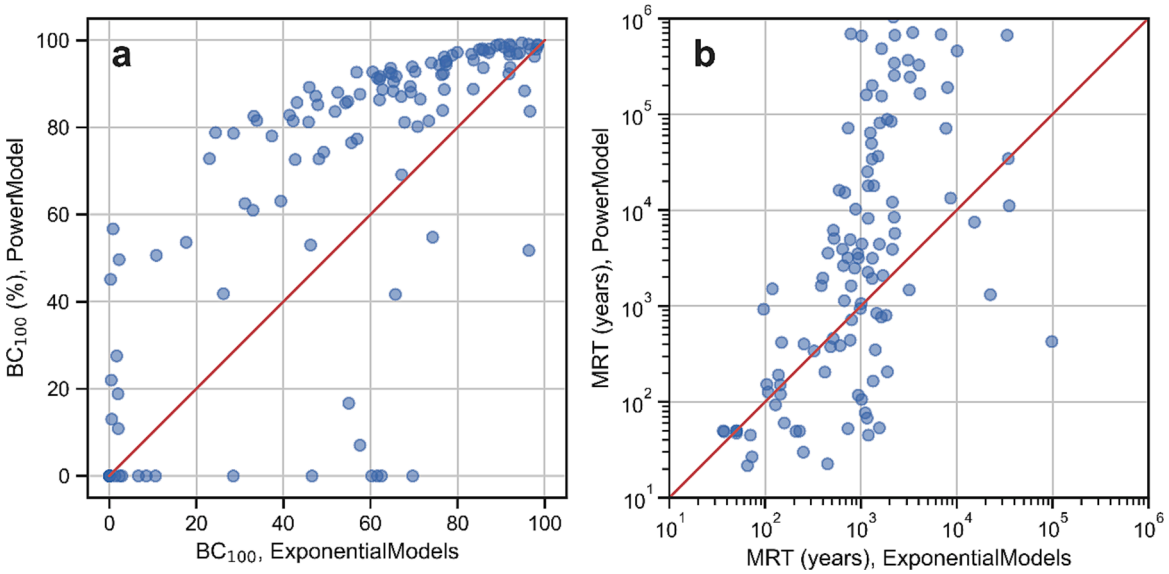

Fig. 6. Comparison between predictions of power model (strategy S3) and exponential models (strategy S2), in terms of a) fraction of biochar C remaining after 100 years (BC_{100}) and b) apparent mean residence time (MRT, years, time after which 63 % of the carbon is lost), at incubation temperature. For some observations, the apparent MRTs calculated with power model were in the range of 10^6 to 10^{10} years (cut-out in panel b), which results from rapidly decreasing decay rates.

Notably, incubation conditions and other pyrolysis conditions exhibited weaker correlations with persistence estimates (around 0.2 to 0.3).

3.4.2. *Correlation between BC_{100} and molar H/C ratio*

Correlation between BC_{100} and H/C ratios at 20 °C is shown in Fig. 7, for both extrapolation via exponential and power model curve fittings. When using power models, the main cluster of observations was contained within 20 % of biochar carbon lost (Fig. 7b), while the variation is twice as high with exponential models (Fig. 7a).

Linear regressions and power-model regressions were both fitted on three different subsets of observations (Table 5, Fig. 7). Regardless of model type and curve fitting approach, removing singular observations and outliers reduced mean absolute error (MAE) but also dramatically increased R^2 values (Table 5), as expected. It is worth noting that singular observations identified in previous modelling steps do not correspond only to observations with very low predicted BC_{100}, but in fact span from 0 to 100 % with the majority of observations in the range 20 %-80 % (data points in grey in Fig. 7). The 4 remaining outliers excluded here correspond to gasification crop biochars with an H/C of 0.5 (Ventura et al., 2019), one slow pyrolysis crop biochar with an H/C of 0.7 produced at 350 °C (Herath et al., 2015), and one slow pyrolysis wood biochar with an H/C of 0.62 studied under field conditions (only for exponential models) (Singh et al., 2015). The gasification biochars and the wood biochar were studied under field conditions, and decay rates stabilized around 4×10^{-2} gC gC_0^{-1} $year^{-1}$, with visible oscillations due to temperature variations. For the gasification biochars, it was also noted that the presence of roots (in a willow cultivated field) increased decomposition (Ventura et al., 2019). All the 4 biochars incubated by Herath et al. (2015) under laboratory conditions lost more than 10 % of carbon within 500 days, with no clear explanation beside the relatively high organic matter content of the two soil types used in those incubations. These outliers call for further field studies but also further characterization of these biochars, to attempt elucidating why their behavior is markedly different from most other observations.

Previous work mainly relied on linear correlations for developing biochar persistence predictions with H/C ratio (Lehmann et al., 2021; Woolf et al., 2021), although a power model was also recently published (Rodrigues et al., 2023). In the case of exponential extrapolation (Fig. 7a), predictions of both power and linear regressions were rather similar for H/C between 0.4 and 1.0. At H/C below 0.4, the power regression reached a plateau while the linear regression extended beyond 100 % (which is then usually capped to 100 %). At H/C above 1.0, the power regression declined more rapidly than the linear regression, before reaching 0 %. Although H/C ratios beyond 1.0 are not relevant for evaluating persistence of biochars (since biochar is usually defined as H/C below 0.7), we noted that by excluding those observations, any previously published linear regressions and the ones produced here would perform much worse in terms of R^2 and MAE and have a very different slope.

In the case of power extrapolation (Fig. 7b), differences between linear and power regressions were more pronounced. Although the R^2 was 0.7, the linear regression did not match the data well, overestimating persistence at low H/C, underestimating it in the middle range of H/C and overestimating it at high H/C. The power model was able to describe the data better, with a plateau for H/C below 0.6, followed by a rapid decline. In practice, this power regression applied to the dataset with power extrapolation implies that all biochars with an H/C between 0 and 0.7 would have a similar predicted BC_{100} (varying between 94 % and 91 %). This outcome should be considered with caution because of the large modelling uncertainty and inherent assumption of power extrapolations in curve fitting. In addition, it should be noted again that persistence estimates for H/C below 0.3 are not sufficiently supported by data (Fig. 4).

Similarly to Rodrigues et al. (2023), we find that the use of power regressions is preferred over linear regressions, for describing 100-year biochar persistence as a function of the H/C ratio. However, we further stress that the data selection, curve fitting, and soil temperature adjustment procedures significantly affect the persistence predictions. For instance, the power regression from Rodrigues et al. (2023) reaches 0 % persistence at H/C of around 0.75. This directly results from i) excluding any observations with H/C above 0.7 despite their relatively high modelled persistence, and from ii) including of a series of observations in the H/C range 0.6–0.7 that in our analysis were excluded because of curve fitting issues or temperature adjustment issues.

3.4.3. *Exploring multi-variate, multi-target random forest regressions*

The random forest regressions were fitted on a subset of observations that excluded singular observations (identified in sections 3.2, 3.3) and remaining outliers identified previously (section 3.4.2), using power model extrapolation. Two thirds of the regression models had an R^2

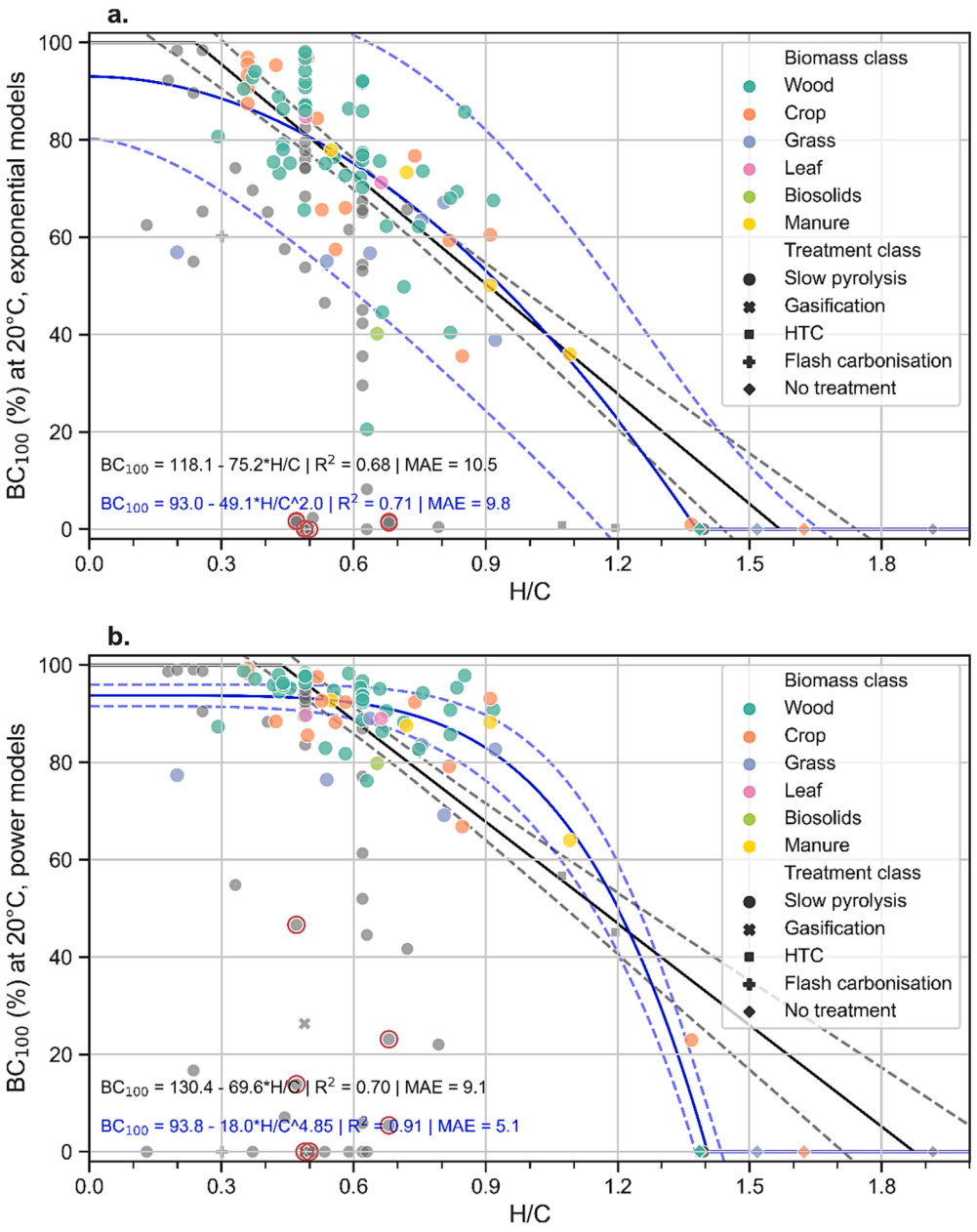

Fig. 7. Biochar carbon remaining after 100-years (BC_{100}) at an incubation temperature of 20 °C as a function of the molar hydrogen-to-carbon (H/C) ratio, for exponential (a) and power (b) extrapolations. The color and shape of the data points indicate the type of biomass and treatment. Data points in grey are singular observations previously identified, which are excluded from the regressions shown. Circled grey data points are outlier observations discussed in the text. Black solid lines are best-fit linear regressions. Blue solid lines are best-fit power regressions. Dashed lines are the 95 % confidence internals calculated via uncertainty propagation. R^2: Coefficient of determination, MAE: Mean absolute error (%).

above 0.7 (Table S5 in SI). The regression that included 24 metadata variables had the second highest R^2 (0.95) and a root mean square error (RMSE) of 4.2 %. This regression likely overfits the data and is not of any practical use due to the high number of variables, but can be used as a benchmark for other models. Interestingly, many regressions with only 1 or 2 input variables could get close enough to this benchmark (Table S5, Section 10 in SI). Most of these included H/C or HTT with one other variable, such as soil organic matter content, hydrogen content, oxygen content, biochar pH or pyrolysis class. The only regression that outperformed the benchmark (R^2 of 0.97) used H/C and soil organic matter content. The random forest that used only H/C ratio as input variable had a R^2 of 0.85 and a root mean square error of 7.9 %, across all time horizons and soil temperatures included. Fig. 8 further illustrates predictions from the random forest, both for exponential and power extrapolations, at multiple time horizons and H/C values. The development and use of such models could be further investigated, e.g. to provide possible insights to drivers of singular observations and outliers.

3.5. *Perspectives on incubation experiments*

Since the seminal work of Spokas (2010) up to the development of methods for inclusion in IPCC inventory guidelines (IPCC, 2019; Woolf et al., 2021), incubation experiments have been the basis for persistence estimates used in biochar research and practice. However, incubation-based approaches are known to not cover all processes that affect biochar persistence and are built on several assumptions.

First, incubation conditions are assumed to be representative of conditions in the field. However, while in the laboratory, temperature

Table 5
Correlation relationships between BC_{100} (%) and molar H/C for different subsets of data, at 20 °C. Relationships from previous studies are also reported at either 20 °C or 14.9 °C. For model comparison, BC_{100} at H/C of 0.7 is calculated. R^2: Coefficient of determination, MAE: Mean absolute error. BC_{100} and MAE are expressed in the same unit (%). NA: Not available.

Extrapolation	Relationship	Data subset and remarks	Equation (BC_{100} in %)	R^2	MAE (%)	BC_{100} (%) at H/C = 0.7
Exponential curve fitting, at 20 °C	Linear	All data (132 observations)	$BC_{100} = 101–64.1 \times H/C$	0.37	18.7	56.1
		Excluding 49 singular observations	$BC_{100} = 111–69.4 \times H/C$	0.43	14.8	62.4
		Excluding 49 singular observations and 4 outliers	$BC_{100} = 118–75.2 \times H/C$	0.68	10.5	65.4
	Power[#]	All data (127 observations)	$BC_{100} = 84.2–50.2 \times H/C^{1.78}$	0.38 (0.17)	17.8	65.6
		Excluding 49 singular observations	$BC_{100} = 86.4–43.4 \times H/C^{2.06}$	0.44 (0.36)	13.9	65.6
		Excluding 49 singular observations and 4 outliers	$BC_{100} = 93.0–49.1 \times H/C^{1.98}$	0.71 (0.49)	9.8	68.8
Power model curve fitting, at 20 °C	Linear	All data (132 observations)	$BC_{100} = 98.3–46.2 \times H/C$	0.14	27.3	66.0
		Excluding 49 singular observations	$BC_{100} = 122–62.7 \times H/C$	0.35	13.5	78.1
		Excluding 49 singular observations and 4 outliers	$BC_{100} = 130–69.6 \times H/C$	0.70	9.1	81.3
	Power[#]	All data (127 observations)	$BC_{100} = 74.6–3.30 \times H/C^{9.38}$	0.23 (0.096)	24.6	74.5
		Excluding 49 singular observations	$BC_{100} = 87.4–8.21 \times H/C^{7.07}$	0.50 (0.36)	10.7	86.7
		Excluding 49 singular observations and 4 outliers	$BC_{100} = 93.8–18.0 \times H/C^{4.85}$	0.91 (0.86)	5.1	90.6
Previous studies						
Exponential curve fitting	Linear	Woolf et al., 2021, at 20 °C, 85 observations	$BC_{100} = 100.6–65.07 \times H/C$	0.32	NA	55.1
	Linear	Woolf et al., 2021, at 14.9 °C, 85 observations	$BC_{100} = 104.45–63.51 \times H/C$	0.33	NA	60.0
	Power	Rodrigues et al., 2023 at 14.9 °C, 77 observations with C ≥ 50 %, H/C < 0.7 and O/C < 0.4	$BC_{100} = 85.4–493.3 \times H/C^{5.9998}$	0.33	NA	27.3

[#] The R^2 value provided in brackets correspond to R^2 calculated for the part of the curve where predicted BC_{100} is not equal to 0%, i.e. removing from the R^2 calculation the observations with H/C ratio larger than ca 1.3 that improve performance of the clipped power model used and increase R^2 values.

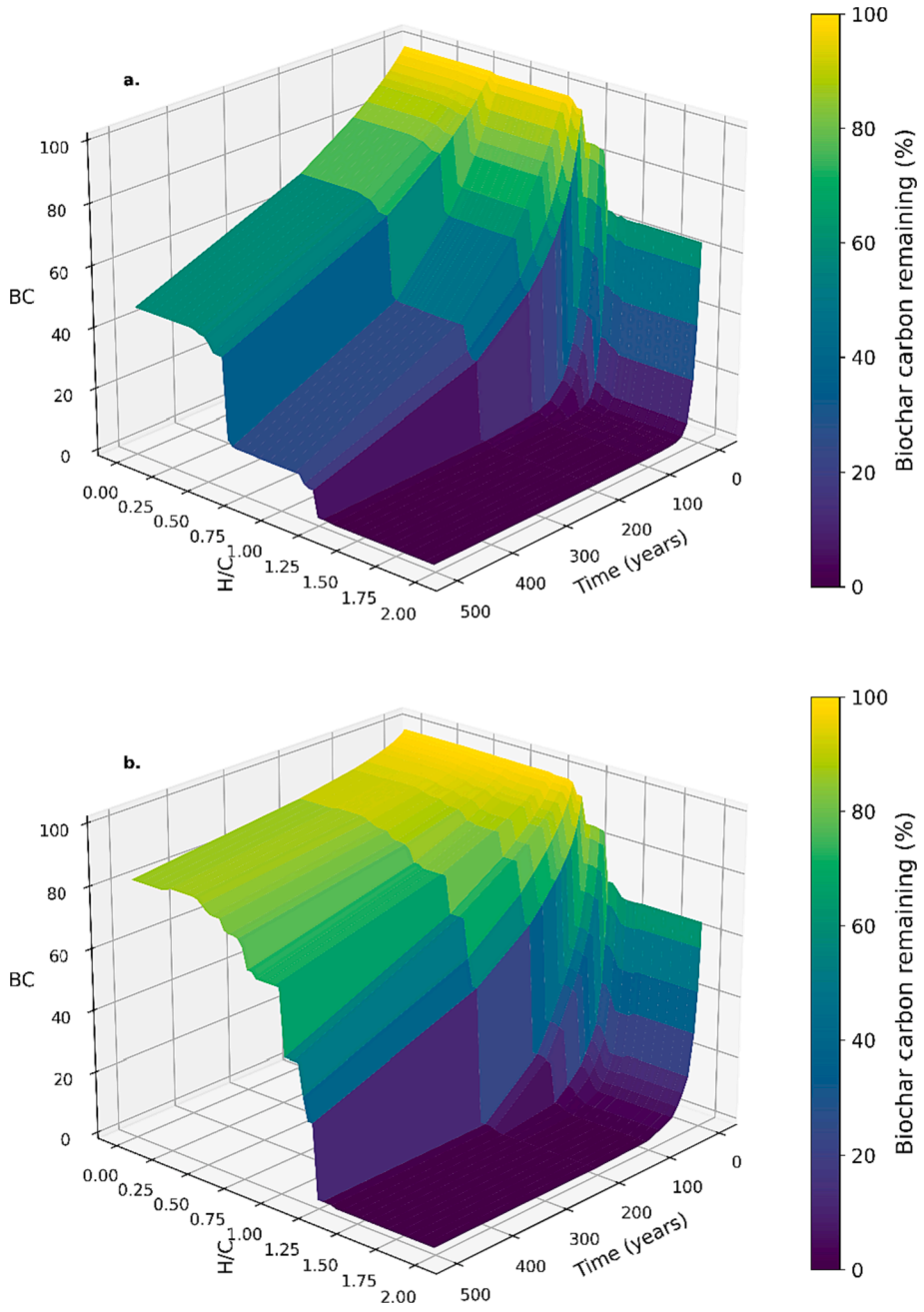

Fig. 8. Biochar carbon remaining (BC) as a function of time (years) and molar H/C ratio, for a soil temperature of 20 °C, as predicted by a random forest algorithm fitted on a subset of observations that excludes singular observations and outliers, extrapolated by (a) exponential or (b) power model curve fitting. The regressions illustrate the use of non-linear multi-target models of biochar persistence.

and moisture are held constant, leading to smooth decay curves, in the field, seasonal variations in decay rates can be observed (Major et al., 2010; Singh et al., 2015; Ventura et al., 2014, 2019). As moisture is controlled at optimal levels for microbial activity, it has been claimed that biochar persistence estimates from laboratory setups are more conservative than field conditions (Kuzyakov et al., 2009). However, due to larger diversity of fungi and fauna, supply of nutrients, the presence of roots, root exudates, extra-cellular enzymes and light, field conditions are also described as more biologically active and could thereby lead to higher decomposition rates (Feng et al., 2023; Ventura et al., 2019). Moreover, under field conditions, soils are often exposed to drying/rewetting cycles as well as freezing-thawing cycles and how these processes affect the environmental fate of biochar is poorly understood (Schimmelpfennig et al., 2017). Studies indicate that certain microorganisms have the ability to degrade even highly condensed aromatic carbon structures such as graphene or graphites, although mineralization rates in soil are low (Liu et al., 2015; Navarro et al., 2020). At the same time, in the field, biochar can be protected from microbial attack via formation of aggregates with soil particles (Burrell et al., 2016). Overall, differences between field and laboratory incubations have not been quantitatively assessed.

Second, biochar is assumed to stay in the upper soil layers, and not migrate via leaching and erosion to deeper soil layers, rivers, and sediments, where decomposition rates are expected to be significantly lower. Movement of pyrogenic carbon in the environment has mostly been studied in the context of vegetation fires and organic carbon presence in rocks, to understand the planetary carbon cycle (Abiven and Santín, 2019; Bird et al., 2015; Bowring et al., 2022). However, it has

also been shown that biochar and pyrogenic carbon can be mobile in soils (Lutfalla et al., 2017; Major et al., 2010). Partial transport of biochar particles away from topsoil could be a significant but variable process resulting in very long-term persistence of biochar carbon and is a process that is not captured by laboratory incubations. The presence of charcoal (as well as biomass) in archaeological artefacts and macerals in geological records is a clear indication that biochar can be preserved for millennia under the right environmental condition (Ascough et al., 2020, 2018). However, the mere existence of such very old organic material is not proof that all biochar applied to a soil will be preserved in this way nor that certain biochar fractions are 'inert'.

Third, the whole biochar carbon pool is assumed to behave according to the assumptions built into the extrapolation model (i.e. single, double, triple exponential, or power decay) and parametrized as observed during incubation. This assumption has recently been a source of critique of persistence estimates derived from incubation, with some arguing that the highly condensed aromatic fractions of biochar are strictly 'inert' (Petersen et al., 2023). However, possible mechanisms of biotic and abiotic alteration of coal and pyrogenic carbon structures are also known (De la Rosa et al., 2018; Liu et al., 2015; Navarro et al., 2020; Sekhohola et al., 2013; Shneour, 1966). It has also been claimed that incubations must be sufficiently long, at least 1 year and preferably 2 years (Lehmann et al., 2021) to yield reliable enough extrapolations. Incubations longer than 2 years usually show a stabilisation of measured decay rates (Fig. 3), but it remains impossible to say whether those rates will be maintained for multiple decades. It is worth noting that long laboratory incubations sometimes lead to reduced microbial activity because of depletion of nutrients or other unknown factors. Nevertheless, we have clarified that different extrapolation models (power vs exponential) make different extrapolation assumptions, and that power models which extrapolate decline in decay rate are partly in line with the theory that biochar is an ensemble of increasingly persistent forms of aromatic carbon.

3.6. Further work

Dataset. More data could be collected from existing studies. In particular, time series from controls were not compiled in the dataset; hence, priming effects were not possible to re-analyse. Likewise, incubations without separate biochar C flux measurement (i.e. studies where priming and biochar decomposition cannot be distinguished from one another) were not included. Since incubation without separate biochar C flux measurement are easier and cheaper to perform, developing reliable-enough predictors of priming during incubations could be a way to expand the usable dataset, albeit with some uncertainties.

Modelling. Refining soil temperature adjustment methods is an important area of work, which would require new studies at low soil temperatures. For curve fitting, techniques to deal with irregularities in data could be developed and applied, e.g. fitting on only a part of the timeseries or excluding some data points. Other types of model functions could be tested, e.g. models with connected or inert pools (Sleutel et al., 2005). The dataset could also be used to inform soil carbon models on including biochar related processes (Pulcher et al., 2022).

New biochar incubations and characterisation. From this work but also other recent research (Howell et al., 2022; Petersen et al., 2023), it appears necessary to conduct new incubations with comparable experimental conditions on labelled biochars with very low H/C ratios, biochars with very high inertinite content, as well as on fractions of biochar remaining after certain thermochemical treatments (Howell et al., 2022; Petersen et al., 2023). Characterisation methods like hydrogen pyrolysis (Ascough et al., 2009; Howell et al., 2022) or random reflectance measurements (Mastalerz et al., 2023; Petersen et al., 2023) ought to be performed in new incubations, but also to the extent possible, performed on biochars from previous incubation studies if samples are still available. Finally, biochar persistence should also be further studied in the biologically active topsoil layer under field conditions, and other environments with high microbial activity, alongside the physical movement of biochar particles away from the topsoil layer.

Policy estimates of biochar persistence and durability of carbon storage. Finally, the consolidation of knowledge on biochar persistence up to the adoption of numbers for use in various policies and carbon finance mechanisms requires, in our opinion, interdisciplinary work aiming at integrating various approaches and co-existing theories. This could lead to the formulation of policy-relevant estimates of biochar carbon storage durability (last step in Fig. 1), whether for use in national inventories or in project-specific carbon accounting, e.g. with adequate conservative margins.

4. Conclusion

An extensive dataset of published biochar decomposition studies was created and is made available alongside a *python* library to conduct reproducible analyses. This is a significant step forward for biochar persistence modelling, as it provides a guide for future experiments, allows the research community to easily extend the dataset, and improves the transparency of resulting models.

The detailed re-analysis performed here does not cast doubts on biochar systems contributing to climate change mitigation via carbon storage, but critically examined the assumptions and modelling techniques associated with persistence estimates derived from incubation studies. Thereby, we were able to validate and refine biochar persistence models but also highlighted their limitations. In particular, it is debatable whether incubation-based approaches are adequate for extrapolating persistence estimates beyond 100 years because short-term incubations do not capture all the processes that are relevant on long time scales.

Ultimately, as other approaches to biochar persistence determination are emerging in other disciplines, e.g. petrogeology, it is critical for transdisciplinary work to begin, aiming to integrate the various approaches and theories. Such an effort is urgently needed due to the rising industry and policy interest for biochar as a climate solution.

Funding

This project was funded by the Swedish Energy Agency, under grant number P2021-00117.

CRediT authorship contribution statement

Elias S. Azzi: Conceptualization, Methodology, Data curation, Software, Formal analysis, Investigation, Visualization, Writing – original draft, Writing – review & editing, Funding acquisition. **Haichao Li:** Writing – review & editing. **Harald Cederlund:** Conceptualization, Funding acquisition, Writing – review & editing. **Erik Karltun:** Funding acquisition, Writing – review & editing. **Cecilia Sundberg:** Conceptualization, Funding acquisition, Methodology, Supervision, Writing – review & editing.

Declaration of competing interest

The authors declare the following financial interests/personal relationships which may be considered as potential competing interests: Elias S. Azzi has worked as independent consultant to the benefit of Puro.earth Oy, in parallel of his research affiliation to the Swedish University of Agricultural Sciences (SLU).

Data availability

Data and code are fully available in a public repository shared in the manuscript (GitHub link).

Acknowledgements

The authors acknowledge the contribution of project partners Helena Söderqvist and Tom Källgren. The authors are grateful to all researchers that have shared data from their incubation studies (Budai, A., Zimmerman, A. R., Cowie, A., Rasse, D., Singh, B. P., Santos, F., Lehmann, J., Fang, Y., Aubertin, M-L.), saving days of digitizing work. Last, the authors also thank all researchers that have contributed indirectly to this work by engaging in a series of calls on the topic of biochar persistence in April-May 2023.

Appendix A–C. Supplementary material

Supplementary data to this article can be found online at https://doi.org/10.1016/j.geoderma.2023.116761.

References

Abiven, S., Santín, C., 2019. Editorial: from fires to oceans: dynamics of fire-derived organic matter in terrestrial and aquatic ecosystems. Front. Earth Sci. 7, 31. https://doi.org/10.3389/feart.2019.00031.

Andrade, C., Albers, A., Zamora-Ledezma, E., Hamelin, L., 2022. Database to determine the Carbon recalcitrance and carbon conversion rate to bioeconomy coproducts. 10.48531/JBRU.CALMIP/WYWKIQ.

Ascough, P.L., Bird, M.I., Brock, F., Higham, T.F.G., Meredith, W., Snape, C.E., Vane, C. H., 2009. Hydropyrolysis as a new tool for radiocarbon pre-treatment and the quantification of black carbon. Quat. Geochronol. 4, 140–147. https://doi.org/10.1016/j.quageo.2008.11.001.

Ascough, P.L., Bird, M.I., Meredith, W., Snape, C., Large, D., Tilston, E., Apperley, D., Bernabé, A., Shen, L., 2018. Dynamics of charcoal alteration in a tropical biome: a biochar-based study. Front. Earth Sci. 6 https://doi.org/10.3389/feart.2018.00061.

Ascough, P.L., Brock, F., Collinson, M.E., Painter, J.D., Lane, D.W., Bird, M.I., 2020. Chemical characteristics of macroscopic pyrogenic carbon following millennial-scale environmental exposure. Front. Environ. Sci. 7 https://doi.org/10.3389/fenvs.2019.00203.

Aubertin, M.-L., Girardin, C., Houot, S., Nobile, C., Houben, D., Bena, S., Brech, Y.L., Rumpel, C., 2021. Biochar-compost interactions as affected by weathering: effects on biological stability and plant growth. Agronomy 11, 336. https://doi.org/10.3390/agronomy11020336.

Bird, M.I., Wynn, J.G., Saiz, G., Wurster, C.M., McBeath, A., 2015. The pyrogenic carbon cycle. Annu. Rev. Earth Planet. Sci. 43, 273–298. https://doi.org/10.1146/annurev-earth-060614-105038.

Bowring, S.P.K., Jones, M.W., Ciais, P., Guenet, B., Abiven, S., 2022. Pyrogenic carbon decomposition critical to resolving fire's role in the Earth system. Nat. Geosci. 15, 135–142. https://doi.org/10.1038/s41561-021-00892-0.

Breiman, L., 2001. Random Forests. Mach. Learn. 45, 5–32. https://doi.org/10.1023/A:1010933404324.

Budai, A., Zimmerman, A.R., Cowie, A.L., Webber, J.B.W., Singh, B.P., Glaser, B., Masiello, C.A., Andersson, D., Shields, F., Lehmann, J., Camps Arbestain, M., Williams, M., Sohi, S., Joseph, S., 2013. Biochar Carbon Stability Test Method : An assessment of methods to determine biochar carbon stability, International Biochar Initiative.

Budai, A., Rasse, D.P., Lagomarsino, A., Lerch, T.Z., Paruch, L., 2016. Biochar persistence, priming and microbial responses to pyrolysis temperature series. Biol. Fertil. Soils 52, 749–761. https://doi.org/10.1007/s00374-016-1116-6.

Burrell, L.D., Zehetner, F., Rampazzo, N., Wimmer, B., Soja, G., 2016. Long-term effects of biochar on soil physical properties. Geoderma 282, 96–102. https://doi.org/10.1016/j.geoderma.2016.07.019.

Canadell, J.G., Monteiro, P.M.S., Costa, M.H., Cotrim da Cunha, L., Cox, P.M., Eliseev, A. V., Henson, S., Ishii, M., Jaccard, S., Koven, C., Lohila, A., Patra, P.K., Piao, S., Rogelj, J., Syampungani, S., Zaehle, S., Zickfeld, K., 2021. Chapter 5: Global carbon and other biogeochemical cycles and feedbacks, in: Climate Change 2021: The Physical Science Basis. Contribution of Working Group I to the Sixth Assessment Report of the Intergovernmental Panel on Climate Change [Masson-Delmotte, V., P. Zhai, A. Pirani, S. L. Connors, C. Péan, S. Berger, N. Caud, Y. Chen,. Cambridge, United Kingdom, and New York, NY, USA.

Chabbi, A., Rumpel, C., Grootes, P.M., González-Pérez, J.A., Delaune, R.D., Gonzalez-Vila, F., Nixdorf, B., Hüttl, R.F., 2006. Lignite degradation and mineralization in lignite-containing mine sediment as revealed by 14C activity measurements and molecular analysis. Org. Geochem. 37, 957–976. https://doi.org/10.1016/j.orggeochem.2006.02.002.

Cheng, C.-H., Lehmann, J., Thies, J.E., Burton, S.D., 2008. Stability of black carbon in soils across a climatic gradient. J. Geophys. Res. Biogeosciences 113. https://doi.org/10.1029/2007JG000642.

Crombie, K., Mašek, O., Sohi, S.P., Brownsort, P., Cross, A., 2013. The effect of pyrolysis conditions on biochar stability as determined by three methods. GCB Bioenergy 5, 122–131. https://doi.org/10.1111/gcbb.12030.

Cross, A., Sohi, S.P., 2013. A method for screening the relative long-term stability of biochar. GCB Bioenergy 5, 215–220. https://doi.org/10.1111/gcbb.12035.

Davidson, E.A., Janssens, I.A., 2006. Temperature sensitivity of soil carbon decomposition and feedbacks to climate change. Nature 440, 165–173. https://doi.org/10.1038/nature04514.

De la Rosa, J.M., Miller, A.Z., Knicker, H., 2018. Soil-borne fungi challenge the concept of long-term biochemical recalcitrance of pyrochar. Sci. Rep. 8, 2896. https://doi.org/10.1038/s41598-018-21257-5.

Elsgaard, L., Eriksen, R.L., 2023. Temperature control on biochar decomposition in soil - implications for long-term carbon sequestration, in: EGU General Assembly 2023, Vienna, Austria, 24–28 Apr 2023, EGU23-9326. 10.5194/egusphere-egu23-9326.

Fang, Y., Singh, B.P., Singh, B., 2014. Temperature sensitivity of biochar and native carbon mineralisation in biochar-amended soils. Agric. Ecosyst. Environ. 191, 158–167. https://doi.org/10.1016/J.AGEE.2014.02.018.

Fang, Y., Singh, B.P., Nazaries, L., Keith, A., Tavakkoli, E., Wilson, N., Singh, B., 2019. Interactive carbon priming, microbial response and biochar persistence in a Vertisol with varied inputs of biochar and labile organic matter. Eur. J. Soil Sci. 70, 960–974. https://doi.org/10.1111/EJSS.12808.

Feng, J., Yu, D., Sinsabaugh, R.L., Moorhead, D.L., Andersen, M.N., Smith, P., Song, Y., Li, X., Huang, Q., Liu, Y.-R., Chen, J., 2023. Trade-offs in carbon-degrading enzyme activities limit long-term soil carbon sequestration with biochar addition. Biol. Rev. 98, 1184–1199. https://doi.org/10.1111/brv.12949.

Glaser, B., Haumaier, L., Guggenberger, G., Zech, W., 2001. The "Terra Preta" phenomenon: a model for sustainable agriculture in the humid tropics. Naturwissenschaften 88, 37–41. https://doi.org/10.1007/s001140000193.

Harper, M., n.d. python-ternary: Ternary Plots in Python. Zenodo 10.5281/zenodo.594435. 10.5281/zenodo.594435.

Harris, C.R., Millman, K.J., van der Walt, S.J., Gommers, R., Virtanen, P., Cournapeau, D., Wieser, E., Taylor, J., Berg, S., Smith, N.J., Kern, R., Picus, M., Hoyer, S., van Kerkwijk, M.H., Brett, M., Haldane, A., del Río, J.F., Wiebe, M., Peterson, P., Gérard-Marchant, P., Sheppard, K., Reddy, T., Weckesser, W., Abbasi, H., Gohlke, C., Oliphant, T.E., 2020. Array programming with NumPy. Nature 585, 357–362. https://doi.org/10.1038/s41586-020-2649-2.

Harvey, O.R., Kuo, L.-J., Zimmerman, A.R., Louchouarn, P., Amonette, J.E., Herbert, B. E., 2012. An index-based approach to assessing recalcitrance and soil carbon sequestration potential of engineered black carbons (biochars). Environ. Sci. Technol. 46, 1415–1421. https://doi.org/10.1021/es2040398.

Herath, H.M.S.K., Camps-Arbestain, M., Hedley, M.J., Kirschbaum, M.U.F., Wang, T., van Hale, R., 2015. Experimental evidence for sequestering C with biochar by avoidance of CO2 emissions from original feedstock and protection of native soil organic matter. GCB Bioenergy 7, 512–526. https://doi.org/10.1111/GCBB.12183.

Howell, A., Helmkamp, S., Belmont, E., 2022. Stable polycyclic aromatic carbon (SPAC) formation in wildfire chars and engineered biochars. Sci. Total Environ. 849, 157610 https://doi.org/10.1016/j.scitotenv.2022.157610.

Hunter, J.D., 2007. Matplotlib: A 2D Graphics Environment. Comput. Sci. Eng. 9, 90–95. https://doi.org/10.1109/MCSE.2007.55.

IPCC, 2018. Summary for Policymakers, in: Masson-Delmotte, V., Zhai, P., Pörtner, H.O., Roberts, D., Skea, J., Shukla, P.R., Pirani, A., Moufouma-Okia, W., Péan, C., Pidcock, R., Connors, S., Matthews, J.B.R., Chen, Y., Zhou, X., Gomis, M.I., Lonnoy, E., Maycock, T., Tignor, M., Waterfield, T. (Eds.), Global Warming of 1.5°C. An IPCC Special Report on the Impacts of Global Warming of 1.5°C above Pre-Industrial Levels and Related Global Greenhouse Gas Emission Pathways, in the Context of Strengthening the Global Response to the Threat of Climate Change,. Switzerland.

IPCC, 2019. 2019 refinement to the 2006 IPCC guidelines for national greenhouse gas inventories [WWW Document]. URL https://www.ipcc-nggip.iges.or.jp/public/2019rf/index.html.

Ippolito, J.A., Cui, L., Kammann, C., Wrage-Mönnig, N., Estavillo, J.M., Fuertes-Mendizabal, T., Cayuela, M.L., Sigua, G., Novak, J., Spokas, K., Borchard, N., 2020. Feedstock choice, pyrolysis temperature and type influence biochar characteristics: a comprehensive meta-data analysis review. Biochar 2, 421–438. https://doi.org/10.1007/s42773-020-00067-x.

Kuzyakov, Y., Subbotina, I., Chen, H., Bogomolova, I., Xu, X., 2009. Black carbon decomposition and incorporation into soil microbial biomass estimated by 14C labeling. Soil Biol. Biochem. 41, 210–219. https://doi.org/10.1016/J.SOILBIO.2008.10.016.

Kuzyakov, Y., Bogomolova, I., Glaser, B., 2014. Biochar stability in soil: Decomposition during eight years and transformation as assessed by compound-specific 14C analysis. Soil Biol. Biochem. 70, 229–236. https://doi.org/10.1016/J.SOILBIO.2013.12.021.

Leal, O. dos A., Dick, D.P., De La Rosa, J.M., Leal, D.P.B., González-Pérez, J.A., Campos, G.S., Knicker, H., 2019. Charcoal Fine Residues Effects on Soil Organic Matter Humic Substances, Composition, and Biodegradability. Agronomy 9, 384. 10.3390/AGRONOMY9070384.

Lehmann, J., Abiven, S., Kleber, M., Pan, G., Singh, B.P., Sohi, S.P., Zimmerman, A.R., 2015. Persistence of biochar in soil. In: Biochar for Environmental Management: Science, Technology and Implementation (2nd Edition). Routledge, London, pp. 235–282.

Lehmann, J., Cowie, A., Masiello, C.A., Kammann, C., Woolf, D., Amonette, J.E., Cayuela, M.L., Camps-Arbestain, M., Whitman, T., 2021. Biochar in climate change mitigation. Nat. Geosci. 14, 883–892. https://doi.org/10.1038/s41561-021-00852-8.

Leng, L., Huang, H., Li, H., Li, J., Zhou, W., 2019a. Biochar stability assessment methods: A review. Sci. Total Environ. 647, 210–222. https://doi.org/10.1016/j.scitotenv.2018.07.402.

Leng, L., Xu, X., Wei, L., Fan, L., Huang, H., Li, J., Lu, Q., Li, J., Zhou, W., 2019b. Biochar stability assessment by incubation and modelling: Methods, drawbacks and recommendations. Sci. Total Environ. 664, 11–23. https://doi.org/10.1016/j.scitotenv.2019.01.298.

Liu, B., Liu, Q., Wang, X., Bei, Q., Zhang, Y., Lin, Z., Liu, G., Zhu, J., Hu, T., Jin, H., Wang, H., Sun, X., Lin, X., Xie, Z., 2020. A fast chemical oxidation method for predicting the long-term mineralization of biochar in soils. Sci. Total Environ. 718, 137390 https://doi.org/10.1016/J.SCITOTENV.2020.137390.

Liu, L., Zhu, C., Fan, M., Chen, C., Huang, Y., Hao, Q., Yang, J., Wang, H., Sun, D., 2015. Oxidation and degradation of graphitic materials by naphthalene-degrading bacteria. Nanoscale 7, 13619–13628. https://doi.org/10.1039/C5NR02502H.

Lutfalla, S., Abiven, S., Barré, P., Wiedemeier, D.B., Christensen, B.T., Houot, S., Kätterer, T., Macdonald, A.J., Van Oort, F., Chenu, C., 2017. Pyrogenic carbon lacks long-term persistence in temperate arable soils. Front. Earth Sci. 5, 1–10. https://doi.org/10.3389/feart.2017.00096.

Major, J., Lehmann, J., Rondon, M., Goodale, C., 2010. Fate of soil-applied black carbon: downward migration, leaching and soil respiration. Glob. Chang. Biol. 16, 1366–1379. https://doi.org/10.1111/j.1365-2486.2009.02044.x.

Mastalerz, M., Drobniak, A., Briggs, D., Bradburn, J., 2023. Variations in microscopic properties of biomass char: Implications for biochar characterization. Int. J. Coal Geol. 271, 104235 https://doi.org/10.1016/j.coal.2023.104235.

McKinney, W., 2010. Data Structures for Statistical Computing in Python. In: van der Walt, S., Millman, J. (Eds.), Proceedings of the 9th Python in Science Conference, pp. 56–61. https://doi.org/10.25080/Majora-92bf1922-00a.

Navarro, D.A., Kah, M., Losic, D., Kookana, R.S., McLaughlin, M.J., 2020. Mineralisation and release of 14C-graphene oxide (GO) in soils. Chemosphere 238, 124558. https://doi.org/10.1016/j.chemosphere.2019.124558.

Nguyen, B.T., Lehmann, J., Hockaday, W.C., Joseph, S., Masiello, C.A., 2010. Temperature sensitivity of black carbon decomposition and oxidation. Environ. Sci. Technol. 44, 3324–3331. https://doi.org/10.1021/es903016y.

Ntonta, S., Mathew, I., Zengeni, R., Muchaonyerwa, P., Chaplot, V., 2022. Crop residues differ in their decomposition dynamics: Review of available data from world literature. Geoderma 419, 115855. https://doi.org/10.1016/j.geoderma.2022.115855.

pandas development team, T., 2020. pandas-dev/pandas: Pandas. 10.5281/zenodo.3509134.

Pedregosa, F., Varoquaux, G., Gramfort, A., Michel, V., Thirion, B., Grisel, O., Blondel, M., Prettenhofer, P., Weiss, R., Dubourg, V., Vanderplas, J., Passos, A., Cournapeau, D., Brucher, M., Perrot, M., Duchesnay, É., 2011. Scikit-learn: Machine Learning in Python. J. Mach. Learn. Res. 12, 2825–2830.

Petersen, H.I., Lassen, L., Rudra, A., Nguyen, L.X., Do, P.T.M., Sanei, H., 2023. Carbon stability and morphotype composition of biochars from feedstocks in the Mekong Delta. Vietnam. Int. J. Coal Geol. 271, 104233 https://doi.org/10.1016/j.coal.2023.104233.

Pulcher, R., Balugani, E., Ventura, M., Greggio, N., Marazza, D., 2022. Inclusion of biochar in a C dynamics model based on observations from an 8-year field experiment. SOIL 8, 199–211. https://doi.org/10.5194/SOIL-8-199-2022.

Rasse, D.P., Budai, A., O'Toole, A., Ma, X., Rumpel, C., Abiven, S., 2017. Persistence in soil of Miscanthus biochar in laboratory and field conditions. PLoS One 12. https://doi.org/10.1371/journal.pone.0184383.

Rodrigues, L., Budai, A., Elsgaard, L., Hardy, B., Keel, S.G., Mondini, C., Plaza, C., Leifeld, J., 2023. The importance of biochar quality and pyrolysis yield for soil carbon sequestration in practice. Eur. J. Soil Sci. 74, e13396.

Santos, F., Rice, D.M., Bird, J.A., Berhe, A.A., 2021. Pyrolysis temperature and soil depth interactions determine PyC turnover and induced soil organic carbon priming. Biogeochemistry 153, 47–65. https://doi.org/10.1007/s10533-021-00767-x.

Santos, F., Bird, J.A., Asefaw Berhe, A., 2022. Dissolved pyrogenic carbon leaching in soil: Effects of soil depth and pyrolysis temperature. Geoderma 424, 116011. https://doi.org/10.1016/j.geoderma.2022.116011.

Schimmelpfennig, S., Kammann, C., Mumme, J., Marhan, S., Bamminger, C., Moser, G., Müller, C., 2017. Degradation of Miscanthus × giganteus biochar, hydrochar and feedstock under the influence of disturbance events. Appl. Soil Ecol. 113, 135–150. https://doi.org/10.1016/J.APSOIL.2017.01.006.

Sekhohola, L.M., Igbinigie, E.E., Cowan, A.K., 2013. Biological degradation and solubilisation of coal. Biodegradation 24, 305–318. https://doi.org/10.1007/s10532-012-9594-1.

Shneour, E.A., 1966. Oxidation of graphitic carbon in certain soils. Science 151, 991–992. https://doi.org/10.1126/science.151.3713.991.

Singh, B.P., Cowie, A.L., Smernik, R.J., 2012. Biochar carbon stability in a clayey soil as a function of feedstock and pyrolysis temperature. Environ. Sci. Technol. 46, 11770–11778. https://doi.org/10.1021/es302545b.

Singh, B.P., Fang, Y., Boersma, M., Collins, D., Van Zwieten, L., Macdonald, L.M., 2015. In situ persistence and migration of biochar carbon and its impact on native carbon emission in contrasting soils under managed temperate pastures. PLoS One 10, e0141560–e. https://doi.org/10.1371/journal.pone.0141560.

Sleutel, S., De Neve, S., Prat Roibás, M.R., Hofman, G., 2005. The influence of model type and incubation time on the estimation of stable organic carbon in organic materials. Eur. J. Soil Sci. 56, 505–514. https://doi.org/10.1111/j.1365-2389.2004.00685.x.

Spokas, K.A., 2010. Review of the stability of biochar in soils: predictability of O: C molar ratios. Carbon Manag. 1, 289–303. https://doi.org/10.4155/cmt.10.32.

Tisserant, A., Cherubini, F., 2019. Potentials, limitations, co-benefits, and trade-offs of biochar applications to soils for climate change mitigation. Land 8. https://doi.org/10.3390/land8120179.

Ventura, M., Zhang, C., Baldi, E., Fornasier, F., Sorrenti, G., Panzacchi, P., Tonon, G., 2014. Effect of biochar addition on soil respiration partitioning and root dynamics in an apple orchard. Eur. J. Soil Sci. 65, 186–195. https://doi.org/10.1111/ejss.12095.

Ventura, M., Alberti, G., Panzacchi, P., Vedove, G.D., Miglietta, F., Tonon, G., 2019. Biochar mineralization and priming effect in a poplar short rotation coppice from a 3-year field experiment. Biol. Fertil. Soils 55, 67–78. https://doi.org/10.1007/s00374-018-1329-y.

Virtanen, P., Gommers, R., Oliphant, T.E., Haberland, M., Reddy, T., Cournapeau, D., Burovski, E., Peterson, P., Weckesser, W., Bright, J., van der Walt, S.J., Brett, M., Wilson, J., Millman, K.J., Mayorov, N., Nelson, A.R.J., Jones, E., Kern, R., Larson, E., Carey, C.J., Polat, \.Ilhan, Feng, Y., Moore, E.W., VanderPlas, J., Laxalde, D., Perktold, J., Cimrman, R., Henriksen, I., Quintero, E.A., Harris, C.R., Archibald, A. M., Ribeiro, A.H., Pedregosa, F., van Mulbregt, P., SciPy 1.0 Contributors, 2020. SciPy 1.0: Fundamental Algorithms for Scientific Computing in Python. Nat. Methods 17, 261–272. 10.1038/s41592-019-0686-2.

Wang, J., Xiong, Z., Kuzyakov, Y., 2016. Biochar stability in soil: Meta-analysis of decomposition and priming effects. GCB Bioenergy 8, 512–523. https://doi.org/10.1111/gcbb.12266.

Weber, K., Quicker, P., 2018. Properties of biochar. Fuel 217, 240–261. https://doi.org/10.1016/j.fuel.2017.12.054.

Weihermüller, L., Neuser, A., Herbst, M., Vereecken, H., 2018. Problems associated to kinetic fitting of incubation data. Soil Biol. Biochem. 120, 260–271. https://doi.org/10.1016/j.soilbio.2018.01.017.

Woolf, D., Amonette, J.E., Street-Perrott, F.A., Lehmann, J., Joseph, S., 2010. Sustainable biochar to mitigate global climate change. Nat. Commun. 1, 56. https://doi.org/10.1038/ncomms1053.

Woolf, D., Lehmann, J., Ogle, S., Kishimoto-Mo, A.W., McConkey, B., Baldock, J., 2021. Greenhouse gas inventory model for biochar additions to soil. Environ. Sci. Technol. 55, 14795–14805. https://doi.org/10.1021/acs.est.1c02425.

Wu, M., Han, X., Zhong, T., Yuan, M., Wu, W., 2016. Soil organic carbon content affects the stability of biochar in paddy soil. Agric. Ecosyst. Environ. 223, 59–66. https://doi.org/10.1016/j.agee.2016.02.033.

Zhu, X., Mao, L., Chen, B., 2019. Driving forces linking microbial community structure and functions to enhanced carbon stability in biochar-amended soil. Environ. Int. 133, 105211 https://doi.org/10.1016/j.envint.2019.105211.

Zimmerman, A.R., 2010. Abiotic and microbial oxidation of laboratory-produced black carbon (Biochar). Environ. Sci. Technol. 44, 1295–1301. https://doi.org/10.1021/es903140c.

Zimmerman, A.R., Gao, B., Ahn, M.-Y., 2011. Positive and negative carbon mineralization priming effects among a variety of biochar-amended soils. Soil Biol. Biochem. 43, 1169–1179. https://doi.org/10.1016/j.soilbio.2011.02.005.

Zimmerman, A.R., Ouyang, L., 2019. Priming of pyrogenic C (biochar) mineralization by dissolved organic matter and vice versa. Soil Biol. Biochem. 130, 105–112. https://doi.org/10.1016/j.soilbio.2018.12.011.

Zimmermann, M., Bird, M.I., Wurster, C., Saiz, G., Goodrick, I., Barta, J., Capek, P., Santruckova, H., Smernik, R., 2012. Rapid degradation of pyrogenic carbon. Glob. Chang. Biol. 18, 3306–3316. https://doi.org/10.1111/j.1365-2486.2012.02796.x.